**Science Of The Total Environment**
August 2019, Volume 677 Pages 142-155
https://doi.org/10.1016/j.scitotenv.2019.04.233
https://archimer.ifremer.fr/doc/00499/61095/



# Groundwater discharge to coastal streams – A significant pathway for nitrogen inputs to a hypertrophic Mediterranean coastal lagoon

David Marine [1, 2, 3, *], Bailly-Comte Vincent [2], Munaron Dominique [1], Fiandrino Annie [1], Stieglitz Thomas [3, 4]

[1] Ifremer, UMR MARBEC (Ifremer, IRD, Université de Montpellier, CNRS), Sète, France
[2] NRE, BRGM, University of Montpellier, Montpellier, France
[3] Aix-Marseille Université, CNRS, IRD, INRA, Coll France, CEREGE, 13545 Aix-en-Provence, France
[4] Centre for Tropical Water and Aquatic Ecosystem Research TropWATER, James Cook University, Townsville, Queensland 4811, Australia

* Corresponding author : Marine David, email address : marine.david@ifremer.fr

**Abstract :**

Near-shore and direct groundwater inputs are frequently omitted from nutrient budgets of coastal lagoons. This study investigated groundwater-driven dissolved inorganic nitrogen (DIN) inputs from an alluvial aquifer to the hypertrophic Or lagoon, with a focus on the Salaison River. Piezometric contours revealed that the Salaison hydrogeological catchment is 42% bigger than the surface watershed and hydraulic gradients suggest significant groundwater discharge all along the stream. Hydrograph separation of thewater flowat a gauging station located 3 km upstream from the Or lagoon combined with DIN historical data enabled to estimate that groundwaterdriven DIN inputs account for 81–87% of the annual total DIN inputs to the stream upstream from the gauging station. A radon mass balancewas performed for the hydrological cycle 2017–2018 to estimate groundwater inflow into the downstream part of the stream. Results showed that (1) DIN fluxes increased by a factor 1.1 to 2.3 between the gauging station and the Salaison outlet, (2) the increase in DINwas due to two groundwater-fed canals and to groundwater discharge along the stream, the latter represented 63–78% of the water flow. This study thus highlights the significance of groundwater driven DIN inputs into the Salaison River, which account for 90% of the annualDINinputs. This is particularly true in the downstreampart of the river,which, on averages, supplies 48% of total DIN inputs to the river. These downstream DIN inputs into the Or lagoon were previously not taken into account in the management of this and other Mediterranean lagoons. The inputs will probably affect restoration processes for many years due to their residence timein the aquifer. This study throws light on a rarely documented source of ‘very-nearshore’ groundwater discharge to coastal streams in water and nutrient budgets of coastal zone ecosystems.

Graphical abstract

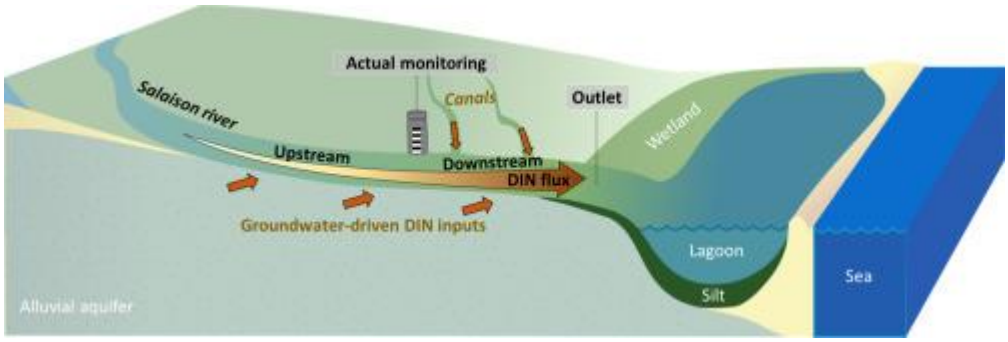


**Highlights**

► Groundwater contribution to nitrogen fluxes was investigated in a major tributary to Or lagoon. ► Groundwater is a major source of dissolved inorganic nitrogen (DIN) for the Salaison River. ► DIN fluxes monitored at the Salaison gauging station are considerably underestimated. ► Groundwater driven DIN inputs should be taken into account in coastal lagoons management actions.

**Keywords** : Groundwater, Nitrogen, Coastal stream, Radon, Lagoon, Land-sea continuum

## 1. Introduction

Transitional water bodies like Mediterranean coastal lagoons are located at the interface between the continent and the sea, they are productive areas which provide substantial ecosystem services (Mooney et al., 2009; Newton et al., 2018). In these semi-enclosed water bodies, the gradient from fresh to saline water creates rich biodiversity which has been documented and protected for several decades now (Basset et al., 2013). As export to the open sea is limited, residence time in these water bodies is sufficiently long to enable assimilation of nutrients by living organisms (Kjerfve and Magill, 1989; Quintana et al., 1998). Coastal lagoons are thus particularly sensitive to nutrient fluxes resulting from anthropogenic activities (de Jonge et al., 2002; Newton et al., 2014). Excess nutrient inputs can lead to eutrophication of the water column, and proliferation of competitive species, thereby upsetting biodiversity equilibrium and reducing the quality of the water (Cloern 2001; Souchu et al. 2010). Among nutrient fluxes, the significant impacts of dissolved inorganic nitrogen (DIN) on eutrophication were already investigated three decades ago (Rimmelin et al., 1998; Taylor et al., 1995).

The main sources of DIN contamination investigated in the past are soil leaching from agricultural land, discharge from wastewater treatment plants (WWTPs), and urban and industrial effluents (Derolez et al., 2014). Indeed, DIN inputs from streams to coastal zones are mostly supplied by surface water, which transports agricultural inputs and wastewater (Meinesz et al., 2013). More recently, groundwater has also been considered as a source of DIN to the coastal zone (Johannes, 1980; Moore, 2010; Rodellas et al., 2015). These studies mainly focussed on direct submarine groundwater discharge (Burnett et al., 2006; Rodellas et al., 2018; Stieglitz et al., 2013) and some demonstrated that inputs from aquifers can significantly contribute to total coastal DIN inputs (Moore, 2010; Slomp and Van Cappellen, 2004). However, the contributions of groundwater inflow to streams discharging in the

immediate coastal environment has rarely been investigated (Martinez et al., 2015; Peterson et al., 2010; Santos et al., 2010).

The goal of the present study was thus to assess inputs of DIN from a coastal aquifer system to a stream discharging into the hypertrophic Or lagoon located in the South of France. This lagoon suffers from recurrent eutrophication which led to a 'bad' ecological status according to the European Union Water Frame Directive (Symbo, 2017). Inputs of DIN from surface waters to the lagoon have been significantly reduced by management actions in the past 20 years, mainly thanks to improvements of wastewater treatment plants and to a lesser extent, to changes in agricultural fertilisation practices. However, despite these actions, no lasting improvement in the quality of the lagoon water has been observed (Derolez et al., 2017). As Salaison River is a perennial stream, groundwater inputs help maintain the water flow in periods with no rainfall, but the associated DIN fluxes have not previously been studied. Regional groundwater has high concentrations of DIN, and, given the comparatively long transit times and associated time lags before discharge, inputs from this coastal aquifer could be an obstacle to restoring Or lagoon.

Different methods are routinely implemented at different scales to study groundwater pathways to streams or to the coastline:

(1) At the aquifer scale, piezometric maps are used to identify drainage pathways, but this method requires a good knowledge of the aquifer geometry and its hydrodynamics properties (Burnett et al., 2001; Schilling and Wolter, 2007).

(2) At the surface watershed scale, hydrograph separation of streamflow data enables surface runoff to be distinguished from groundwater discharge (Chapman, 1999; Eckhardt, 2005; Schilling and Wolter, 2001). However, in coastal rivers, most gauging stations collecting such data are located a few kilometers upstream from the outlet to

avoid the influence of the tide, which can lead to the underestimation of total inputs to the coastline (Santos et al., 2010).

(3) At a smaller scale, natural groundwater tracers like radon and radium are widely used to locate and quantify groundwater discharge into streams (Cook et al., 2003; Mullinger et al., 2007). High concentrations of these radionucleides are naturally found in groundwater whereas low concentrations are found in surface waters, making them efficient tracers of groundwater origin (Burnett and Dulaiova, 2003; Charette et al., 2001). Groundwater flow can be quantified using a mass balance along the stream (Cook et al., 2006; Peterson et al., 2010).

Even though combining approaches to improve our knowledge of the interactions between the aquifer and the coast would seems obvious (Burnett et al., 2001; Martinez et al., 2015), in the past, these methods were usually applied separately (Banks et al., 2011; Burnett et al., 2006; Menció et al., 2014). In the present study, the three approaches were combined to locate and quantify groundwater contribution to DIN inputs in Salaison River. In particular, groundwater inputs were investigated in the section of the stream close to the outlet, downstream from the Salaison gauging station. The three methods were combined to (i) obtain a more holistic view of the hydrogeological functioning of this coastal stream than is possible using a single method, (ii) estimate the groundwater contribution to the Or lagoon via the Salaison River, and (iii) assess more accurate DIN fluxes to the Or lagoon than estimated at the Salaison River gauging station.

## 2. Material and methods

### 2.1. Study sites

#### 2.1.1. Or lagoon

The Or lagoon is located southeast of the city of Montpellier on the French Mediterranean coast (**Fig. 1a**). The surface area of the lagoon is 29.6 km² and the average depth is 1 m. In addition

74 to the presence of an east-west salinity gradient, the lagoon is subject to marked interannual
75 variations in salinity (from 2 to 35 psu). The northern bank of the lagoon is at the edge of 20
76 km² of wetlands which have been the subject of major land reclamations actions. The Or lagoon
77 watershed covers 410 km², and has a flat landform rising from 0 (sea level) to 193 m asl (Blaise
78 et al., 2008). The area is characterised by a typical Mediterranean climate. Precipitation is very
79 low in summer, but intense rainfall events in spring and autumn can cause serious flooding.
80 Annual average precipitation ranges from 600 mm in the southern part of the watershed to 750
81 mm in the northern part (Aquascop, 2013). The area is urbanized but agriculture still represents
82 a major land use with intensively managed vineyards, market gardening, orchards and cereal
83 crops. These activities have led to significant nutrient loading of the underlying aquifer, for
84 example, nitrate concentrations reach 1600 µmol.$L^{-1}$ (i.e. 100 mg($NO_3$)/L) in the eastern part
85 of the aquifer (ADES database http://ades.eaufrance.fr).

86 The Or lagoon lies on a Holocene clay and clayey sand formation and is bound to the north by
87 the coastal plain of Mauguio-Lunel (**Fig. 1a**). The adjacent Villafranchien aquifer is formed by
88 the most recent layers of alluvial and colluvial deposits from the Pliocene and the Holocene,
89 overlying a cretaceous and Jurassic limestone bedrock (Blaise et al., 2008). This aquifer
90 outcrops over 252 km², it is limited to the west by the Lez River and to the east by the Vidourle
91 River, and is partly fed by limestone (karst aquifer) along its north boundary. The aquifer is
92 unconfined, except downstream at the edge of the lagoon where it becomes confined as it
93 expands under Holocene silt. The presence of impermeable silt and clay from the Holocene
94 prevents direct exchanges of water between the aquifer and the lagoon, but to date, little is
95 known about the possible connections through the perennial streams which drain the aquifer
96 (Blaise et al., 2008).

97 ### 2.1.2. Salaison River

98 The Or lagoon is supplied with freshwater from natural streams and artificial canals (**Fig. 1a**).
99 In the eastern watershed, the Lunel and Rhône to Sète canals bring water from the eastern
100 alluvial plain. The present study focusses on the northern part of the watershed, where natural
101 streams flow into the lagoon. Five main rivers and ten temporary streams flowing in a north-
102 west south-east direction discharge into the Or lagoon. The Salaison River is one of the main
103 tributaries flowing into the lagoon, which accounts for 59% (2015-2016) of the total freshwater
104 supplied by the streams in the watershed (Colin et al., 2017). The Salaison River drains a 66
105 $km^2$ watershed which corresponds to 17% of the northern watershed of the Or lagoon. The
106 source of the river is located on the northern Cretaceous limestone and, for its last nine
107 kilometers, it flows over the Villafranchien aquifer.

108 The Salaison River used to receive effluents from four waste water treatment plants (WWTPs)
109 (St Vincent de Barbeyrargues, St Aunes, Vendargues, Mauguio, with a total of 53 800
110 population equivalent) (Aquascop, 2013). In order to reduce inputs to Salaison and Or lagoon,
111 St Vincent de Barbeyrargues WWTP (800 population equivalent) has not released any
112 discharge into the Salaison since 2010, and the three other WWTP outlets were removed from
113 the river between 2008 and 2011 (Symbo, 2014). Since then, diffuse surface and groundwater
114 flows have been the sources of nitrogen inputs into the stream. In addition, the river is fed in
115 its downstream part by two canals, one of which (Balaurie) used to receive effluent from the
116 Vendargues WWTP (6 000 population equivalent) before it was removed and the other
117 (Roubine) was used for urban and storm water drainage (**Fig. 1b**) .

118 ## 2.2. Groundwater catchment of the Salaison river

119 A piezometric survey of the aquifer was carried out to identify the Salaison groundwater
120 catchment, i.e. the area of the aquifer that interacts with the stream. Water levels were measured
121 at 18 piezometers in high water table conditions on May 2nd and 3rd 2018 (**Fig. 1b**). Relative

122 water level data were combined with the stream elevation and a digital elevation model to
123 obtain the piezometric contours around the Salaison River by interpolation in ArcGIS.
124 Groundwater contours based on water table crests on both sides of the Salaison River were
125 used to delineate the Salaison's groundwater catchment.

126 **2.3. Salaison gauging station**

127 Since 1986, stream water flow has been monitored through high-frequency limnimetric
128 measurements made by the Regional Department for Environment, Development and Housing
129 (French acronym DREAL). The gauging station is located 3 km upstream from the outlet to
130 the lagoon and upstream from the Balaurie and Roubine canals (**Fig .1b**), capturing 75% of its
131 total watershed (i.e. 50 $km^2$). Since 2006, DIN concentrations have been sampled by
132 management agencies every two weeks under regular monitoring and at greater frequencies
133 during floods, to assess DIN fluxes at the gauging station.

134 **2.4. Combined methods upstream and downstream from the gauging station**

135 In this study, two sections of the stream were distinguished based on the location of the gauging
136 station: upstream and downstream sections. In the upstream section, the contributions of
137 groundwater to the total DIN inputs at the gauging station were investigated. In the downstream
138 section, additionnal inputs occuring between the gauging station and the Salaison outlet were
139 also investigated, including the two downstream canals, along with groundwater contribution.

140 In any part of the stream, instantaneous DIN fluxes $f_X(t)$ (in $\mu mol.s^{-1}$) were estimated as the
141 product of water flow $Q_X(t)$ (in $L.s^{-1}$) and DIN concentration $[N]_X(t)$ (in $\mu mol.L^{-1}$) (eq. 1) :

142 $$\boldsymbol{f_X(t) = Q_X(t).[N]_X(t)} \quad \mathbf{(1)}$$

143 In the rest of the paper, the time increment '(t)' was removed for the purpose of clarity (i.e. $f_X$,
144 $Q_X$ and $[N]_X$).

First, total DIN fluxes were assessed in each section. Then, estimating groundwater driven DIN fluxes enabled to obtain the groundwater contribution to the total DIN fluxes. The two sections of the stream were approached differently (**Table 1**):

- the upstream part was investigated using historical data collected from 2013 to 2018 at the gauging station, to estimate total DIN fluxes $f_{station}$ and groundwater driven DIN flux $f_{gw}$ (detailed in section **2.5**),
- Supplementary field data were collected in the hydrological cycle 2017-2018 for the downstream section, to estimate additional DIN fluxes $\Delta f_{downstream}$ and additional groundwater driven DIN fluxes $\Delta f_{gw}$ using a radon mass balance (detailed in section **2.6**),

Instantaneous DIN fluxes $f_X$ were integrated over one hydrological year (from September 1$^{st}$ to the following August 31$^{st}$) and converted into tonnes to estimate annual DIN inputs $F_X$ (in tN.y$^{-1}$). The relative groundwater contribution to the total DIN flux was estimated as the ratio of groundwater driven DIN flux to total DIN flux.

## 2.5. Groundwater contribution to DIN fluxes upstream from the Salaison gauging station

### 2.5.1. Water flow at the gauging station

Stream water flow data $Q_{station}$ at the gauging station (**Fig. 1b**) were extracted for the past five hydrological cycles from the DREAL database (hydro.eaufrance.fr, station Y3315080, 2013 - 2018) at hourly intervals, taking into account the fact that the Salaison has a fast hydrological response to rainfall (less than 6 hours between a rainfall event and an increase in flow).

### 2.5.2. DIN fluxes at the gauging station

Dissolved inorganic nitrogen (DIN) concentrations were extracted from the public water quality database Naïades (http://naiades.eaufrance.fr/). A total of 81 DIN data were collected from 2013 to 2018 and clustered according to their associated water flow to assess mean

nutrient concentrations for three water flow classes $[N]_{station}$ (**Table 2**). The DIN flux at the gauging station $f_{station}$ is obtained using eq. 1 with $Q_{station}$ and the associated average DIN class concentrations $[N]_{station}$. Standard variations in DIN concentrations in each of the three classes were used to estimate uncertainty.

### 2.5.3. Groundwater flow at the gauging station

Groundwater flow $Q_{gw}$ was obtained from hydrograph separation of the stream water flow $Q_{station}$. The Chapman model (Chapman, 1999) separates fast subsurface flow from base flow, the latter usually being driven by groundwater. The FlowScreen R package with the function bf_oneparam was used to assess time series of groundwater flow at an hourly time step. The recession constant was estimated for each hydrological cycle using the ESPERE tool (BRGM, Lanini et al. 2016), ($\mu$= 0.971, $\sigma$= 0.019, n=5).

### 2.5.4. Groundwater end-member for DIN concentrations at the gauging station

Three sets of data were collected to determine the groundwater end-member for DIN concentration at the gauging station $[N]_{gw\_s}$ :

- piezometer P4 was sampled for groundwater DIN concentrations on March 8$^{th}$, April 27$^{th}$, May 5$^{th}$, June 25$^{th}$ and July 27$^{th}$ in 2018. In this study, this well was assumed to be representative of the groundwater characteristics because of its location close to the gauging station (**Fig.1b**). In addition, piezometer St Aunes, located upstream of the Salaison watershed, was sampled on March 8$^{th}$, June 25$^{th}$ and July 27$^{th}$ in 2018. For each sample, *in situ* salinity was measured using a multiparameter probe (WTW 3620).
- past DIN concentrations in groundwater at the P4 piezometer were taken from the BRGM study in 2006-2007 (Blaise et al., 2008). These past data were compared with new data to quamify changes in DIN concentrations over the past decade.
- stream data for DIN concentration and conductivity at the gauging station were also used to determine the groundwater end-member.

## 2.6. Groundwater contribution to DIN fluxes downstream from the Salaison gauging station

### 2.6.1. Water inflow downstream from the gauging station

#### 2.6.1.1. Use of a radon and water balance to assess total and groundwater flow

A combined water and radon mass balance was constructed in the downstream part of the stream using two successive box models (**Fig. 2**) to estimate, for the hydrological cycle 2017-2018, (1) the additional groundwater discharge $\Delta Q_{gw}$ and (2) the total additional water flow $\Delta Q_{downstream}$ discharging between the gauging station and the outlet.

The first box for the radon mass balance includes the first 700 m downstream from the gauging station with the discharge from the Balaurie canal, and the second box, the section from 700 m to 2000 m, taking the discharge from the Roubine canal into account (**Fig. 1c**). The final section (2000 m-3000 m downstream from the gauging station) is affected by changes in lagoon water surface level caused by variations in wind and atmospheric pressure, as indicated by variable salinity. The last section can consequently not be considered as being in a steady state. Geological data showed that this section receives a negligible inflow of groundwater due to the impermeability of the underlying silt (**Fig. 1c**), it was not included in the model.

Data were collected when no rain had fallen in the two preceding days. In these dry hydrological conditions, surface runoff was assumed to be negligible in the mass balance and other than the two canals discharging into the boxes, no surface water inputs were taken into consideration. Since all field measurement were completed within a few hours, evaporation of stream water and precipitation were assumed to be negligible in the mass balance. In this case, only groundwater ($\Delta Q_{gw}$) and canals ($Q_{can}$) composed the total water inflow downstream $\Delta Q_{downstream}$ (eq. 2) :

$$\Delta Q_{downstream} = \Delta Q_{gw} + Q_{can} \quad (2)$$

In these conditions, the stream was assumed to be in a steady state with respect to radon. Hyporheic fluxes were also included in the groundwater flow. The estimated groundwater discharge $\Delta Q_{gw}$ includes groundwater *sensu stricto* and hyporheic flux (Avery et al., 2018). The concentration of radon in a box was assumed to be the average concentration of radon in the inflow and the outflow (**Fig. 2**).

#### 2.6.1.2. Radon sampling and analysis

Radon source and sinks used in the mass balance are summarised in **Table 3**. Next, we describe in detail the methods applied to measure radon concentrations in water, diffuse radon inputs from sediments, and atmospheric evasion.

Water was sampled once a month from January to July 2018 at five stations in the stream at 0, 50, 700, 750, 1 850 and 2 000 m downstream from the gauging station and in the two canals (**Fig. 1c**). Groundwater was sampled during the same period at piezometers P4 and St Aunes (same sampling as section 2.5.4). Water was sampled 20 cm below the surface using an immersed pump and primed directly into 2L bottles, thereby ensuring that the water sampled did not exchange any gas with the atmosphere. Conductivity of the sampled water was measured with a WTW 3620 multiparameter probe.

Radon in the samples was analysed using an electronic Radon-in-air monitor (Rad7, Durridge Co.). $^{222}Rn$ was extracted from the water by continuous recirculation of air in a closed loop until it reached equilibrium. Equilibrium values in air were corrected to in-water values using standard methods (Burnett and Dulaiova, 2003; Stieglitz et al., 2013) (**Table 3**).

In order to determine diffuse inputs of radon, sediments were sampled from the bed of the Salaison River and incubated in a 2 L bottle filled with water (average dry weight: 11.92 g, $\sigma$=0.98, n=4) (Stieglitz et al., 2013). Samples were analysed with a Rad7 one month after being collected, when the sediments were assumed to be in equilibrium with the water, i.e. radon

production equals radon loss by decay (Cook et al., 2008). The radon production rate can be estimated as follows (eq. 3):

$$Fdiff = Ceq.\lambda.\frac{Rinc}{Rfield} \quad (3)$$

where $C_{eq}$ is the concentration of radon at equilibrium ($Bq.m^{-3}$), $R_{inc}$ and $R_{field}$ are the ratios of the volume of water to that of the sediment in the incubated sample and in the field, respectively. Average sediment depth was estimated at 0.4 m based on field observations. Average radon diffusion ($F_{diff}$) was calculated to be 600 ± 150 $Bq.m^{-2}.d^{-1}$ (n = 6).

Khadka et al. 2017 developed a method to assess atmospheric evasion at a known water temperature, density and velocity. Using this method in our study, atmospheric evasion (k) ranged between 1.6 $10^{-5}$ to 2.5 $10^{-5}$ $m.s^{-1}$ across the campaigns and was assumed to be constant in the stream for each campaign.

In each sampling campaign, water flow was gauged manually at the gauging station $Q_{station}$ and in the two canals $Q_{can}$ as water flow inputs to the mass balance (**Table 3**). In addition, water flow at the Salaison outlet was gauged manually to validate the model outputs $\Delta Q_{downstream}$ with differential gauging.

To understand the link between groundwater inflow and groundwater dynamics and hydrological conditions, daily time series of water table fluctuation were obtained from the Saint Aunes piezometer on the ADES database (http://ades.eaufrance.fr / ID number BSS 09915X0181/AUNES), and annual rainfall data from the Meteo France database (Fréjorgues weather station).

### 2.6.2. DIN sampling and analysis downstream from the gauging station

At the same time as water was sampled for radon analysis, water was sampled to measure the concentration of DIN in the stream, the two canals and at piezometers P4 and St Aunes as described above in section 2.6.1.2 (**Fig 1c**).

Water samples were taken in HDPE 100 mL bottles, previously washed with analytical grade HCl 1.2N and rinsed with ultrapure water (UW) at the laboratory. All the sampling equipment and filters were rinsed with native water before sampling. Samples were filtered through a 100 µm filter for nitrate ($NO_3$), nitrite ($NO_2$), ammonium ($NH_4$), to prevent particles from interfering with the analysis of dissolved nutrients. Samples were immediately stored at -25°C until analysis. The concentrations of the 3 forms of dissolved inorganic nitrogen were measured using SEAL AA3 Analytical Autoanalyzers using the method described in Aminot and Kerouel (2007) with colorimetric detection (from SEAL Analytical, Germany) and fluorimetric detection (from JASCO, FP-2020plus, France) respectively for, $NO_2$/$NO_3$ and $NH_4$. NID concentration was the sum of nitrites, nitrates and ammonium concentrations for each sample. Analytical grade standards $KNO_3$, $NaNO_2$, $(NH_4)_2SO_4$ were obtained from Sigma-Aldrich (St. Quentin Fallavier, France). Stock standard solutions were prepared in UW and stored in waterproof HDPE bottles at room temperature in the dark at the laboratory. Fresh working standards and calibration solutions were prepared daily by appropriate dilution of the stock solutions using gravimetric procedures. Laboratory quality controls (QC) were performed daily using gravimetric procedures and CertiPUR® NIST solutions (Merck, St-Quentin-en-Yvelines, France), to validate each analysis. The linearity of the calibration curves was always greater than $R^2 = 0.9996$. The limits of detection (LOD) were 0.05, 0.25 and 0.05 µmol.$L^{-1}$ for respectively, $NO_2$, $NO_3$ and $NH_4$.

### 2.6.3. Estimation of annual DIN inputs downstream from the gauging station

The DIN flux at Salaison outlet was estimated as the sum of the DIN flux upstream and downstream, assuming negliglible in-stream nitrogen consumption (i.e. $f_{station} + \Delta f_{downstream}$). The increase factor $\phi_N$ between the DIN flux at the Salaison gauging station $f_{station}$ and the DIN flux at the outlet was estimated as follows (eq. 4):

$$\phi_N = \frac{f_{station} + \Delta f_{downstream}}{f_{station}} \quad (4)$$

Annual increase factor $I_N$ was estimated for each hydrological year from 2013-2014 to 2017-2018 using the frequency of each water flow class in each hydrological year.

### 2.6.4. Groundwater driven DIN fluxes downstream from the gauging station

In the downstream part of the river, assuming negligible additional surface fluxes (2.3.1), DIN fluxes $\Delta f_{downstream}$ were assumed to be the sum of groundwater-driven DIN fluxes $\Delta f_{gw}$ and canal DIN fluxes $f_{can}$ (eq. 5):

$$\Delta f_{downstream} = \Delta f_{gw} + f_{can} \quad (5)$$

The relation between DIN and radon concentrations in the stream was used to determine the groundwater end-member downstream $[N]_{gw\_d}$.

## 3. Results

### 3.1. Groundwater catchment of the Salaison River

The groundwater catchment i.e. the part of the aquifer connected to the Salaison River delineated by the piezometric crest on both sides of the river covers 32.9 km², which is 42% bigger than the Salaison watershed (i.e. surface water catchment) (**Fig. 3**). Piezometric contours show a main channel flowing from the north west to the south east of the aquifer underlying the stream, suggesting significant interactions between surface and groundwater. The contours suggest that on the most upstream part, water inflows from the stream to the aquifer, and downstream, the aquifer discharges into the stream. Along the last 4 km of the stream (i.e. where groundwater feeds the Salaison River), the hydraulic gradient decreases from 0.46 % upstream from the gauging station to 0.15 % downstream. Groundwater discharge may consequently be significant all along the downstream part of the Salaison River. Combined with the geological data, which revealed impermeable sediment units close to the lagoon, the decreasing hydraulic gradient showed that submarine discharge to the lagoon must be negligible, confirming previous conclusions.

### 3.2. Groundwater contribution to DIN fluxes upstream from the Salaison gauging station

Annual DIN inputs at the gauging station ($F_{station}$) ranged from 4.5 ± 1.8 $tN.y^{-1}$ for the dry hydrological cycle 2013-2014 to 55.2 ± 20.1 $tN.y^{-1}$ for the wet hydrological cycle 2014-2015 (**Fig. 4**), with 30.5 ± 11.1 $tN.y^{-1}$ for the hydrological cycle 2017-2018. DIN inputs were linked to annual precipitation (360 mm in 2013-2014; 1176 mm in 2014-2015). Nitrate ($NO_3$) was the main nitrogen form in the stream, with 74% to 99% of the total DIN concentrations.

In 2018, concentrations of DIN in the P4 well ranged around 600 $\mu mol.L^{-1}$ and reached higher values in the St Aunes piezometer (around 800 $\mu mol.L^{-1}$) (**Fig. 5**). Concentrations in the piezometer P4 remained in the same range in the three sampled years, suggesting that

groundwater concentrations can be considered constant in the piezometer close to the Salaison River for the last five hydrological cycles. A correlation found between DIN concentrations at the station and specific conductivity (from DREAL) from 2013 to 2018, suggests that the DIN in the Salaison River originated from a high conductivity end-member (likely to be the 'theorical' groundwater end-member), diluted by mixing with a low DIN/ low conductivity end-member (**Fig. 5**). The latter end-member is likely to be surface runoff water since other DIN sources are negligible (section 2.1.2). Moreover, nitrate composed 95% to 100% of the total DIN forms in P4 and St Aunes and these proportions were similar in the stream. These results suggests that the highly enriched Villafranchien aquifer constitutes the main DIN source in the river.

In the upstream part of the Salaison River, the non-linear correlation between DIN concentrations and conductivity suggests that DIN in the stream cannot be the result of a conservative mixing between two end-members (**Fig. 5**). Based on high DIN concentrations / high conductivity measurements in the stream, the 'effective' groundwater end-member DIN concentrations are twice lower than DIN concentrations measured in the groundwater. The 'theoretical' groundwater end-member for DIN concentration is then reduced to the 'effective' groundwater end-member, suggesting nitrogen assimilation in the stream (i.e. from 600 $\mu mol.L^{-1}$ to 300 $\mu mol.L^{-1}$). To estimate groundwater driven DIN inputs at the gauging station, this 'effective groundwater' end-member was used, i.e. a DIN concentration of 300 ± 100 $\mu mol.L^{-1}$ was assigned to $[N]_{gw\_s}$.

The annual DIN flux from groundwater at the gauging station $F_{gw}$ derived from hydrograph separation $Q_{gw}$ and 'effective' groundwater concentration $[N]_{gw\_s}$ (in eq. 1) ranged from 3.9 ± 1.3 $tN.y^{-1}$ (2013-2014) to 44.8 ± 14.9 $tN.y^{-1}$ (2014-2015) (**Fig. 4**), with 25.9 ± 8.6 $tN.y^{-1}$ for 2017-2018.

Annual groundwater contributions to instream DIN inputs ranged from 81% (2014-2015) to 87% (2013-2014), and 85% in 2017-2018. Contributions were lower for wet hydrological cycles when surface runoff was more important, but annual groundwater contributions were important as groundwater is a major DIN source in the stream. Thus, significant groundwater-driven DIN fluxes are discharged upstream from the gauging station in this perennial stream.

### 3.3. Interannual DIN fluxes downstream from the Salaison gauging station

#### 3.3.1. Interannual water inflow derived from the radon mass balance

Radon concentrations at piezometer P4 and St Aunes were sampled at maximum and minimum table levels (from 14.5 to 16 masl at St Aunes), and ranged from 8 087 ± 178 to 12 412 ± 232 $Bq.m^{-3}$ for P4 and 6 617 ± 327 $Bq.m^{-3}$ to 8 580 ± 215 $Bq.m^{-3}$ for St Aunes. Radon concentrations were in the same range for the two piezometers, and radon concentrations at the P4 piezometers were used as the end-member concentration in the radon mass balance for each campaign (**Table 3**).

Radon concentrations in the stream at the gauging station ranged from 751 $Bq.m^{-3}$ in January to 1 378 $Bq.m^{-3}$ in June, suggesting a considerable inflow of groundwater already occurring upstream from the gauging station (**Fig. 6**). Importantly, radon concentrations increased downstream from the gauging station, indicating significant groundwater influx. The increase in radon concentration is evidence for direct groundwater discharge along the stream, consistent with the geology in this section (**Fig. 3**).

Downstream water flow $\Delta Q_{downstream}$ estimated from the radon mass balance ranged from 55 ± 17 $L.s^{-1}$ in July to 230 ± 73 $L.s^{-1}$ in January (**Fig. 7**). At the Salaison outlet, confidence intervals for water flow estimated with the radon mass balance overlapped those of manual gauging, which enabled to validate the model outputs. Groundwater discharge estimated from the radon mass balance downstream from the gauging station $\Delta Q_{gw}$ ranged from 43 ± 16 $L.s^{-1}$ in July to

375 153 ± 53 $L.s^{-1}$ in January, and contributed between 63% in April (high flows) and 78% in July
376 (low flows) to the total additional discharge $\Delta Q_{downstream}$. The radon mass balances were carried
377 out in different hydrological conditions (from 58 $L.s^{-1}$ to 825 $L.s^{-1}$ at the gauging station) but
378 the confidence interval remained in the same order of magnitude in most of the campaigns. The
379 absolute water flow discharging downstream, with significant uncertainties, did not seem to be
380 correlated (in a simple way) with the water table or with water flow at the gauging station
381 $Q_{station}$. Nevertheless, discharge downstream from the gauging station can have a significantly
382 impact on the water flow reaching the Salaison outlet, especially in dry conditions. For example
383 in July, downstream water discharge $\Delta Q_{downstream}$ increased water flow at the gauging station
384 $Q_{station}$ from 58 $L.s^{-1}$ to 113 $L.s^{-1}$ at the outlet.

385 **3.3.1. Annual DIN inputs downstream**

386 The relative increase in the DIN flux between the gauging station and the outlet $\phi_N$ was
387 inversely correlated with the hydrological conditions (**Fig. 8**). When the water flow was low at
388 the gauging station (dry conditions in July), the groundwater driven DIN flux downstream from
389 the gauging station significantly increased the DIN flux at the Salaison outlet to a factor 2.3 ±
390 0.2. Conversely, in wet hydrological conditions (April), water flow at the outlet increased by a
391 factor 1.1 ± 0.1. Absolute downstream DIN inputs remained in the same order of magnitude
392 but, depending on the hydrological conditions, these inputs may have a significant influence
393 on DIN flow at the outlet.

394 The annual increase factor $I_N$ extrapolated from frequency-weighted water flow classes ranged
395 from 1.8 ± 0.4 in 2014-2015 (in wet conditions) to 2.3 ± 0.6 in 2013-2014 (in dry conditions),
396 and 1.9 ± 0.5 in 2017-2018. Annual DIN fluxes discharged directly into the downstream part
397 of the Salaison River $\Delta F_{downstream}$ estimated with the annual increase factor $I_N$ ranged from 5.6
398 ± 1.4 $tN.y^{-1}$ (2013-2014) and 43.1 ± 20.1 $tN.y^{-1}$ (2014-2015), and 28.1 ± 10.3 $tN.y^{-1}$ in 2017-
399 2018.

### 3.3.2. Contribution of groundwater to the interannual DIN flux downstream

On the downstream part of Salaison River, the positive correlation between DIN and radon concentrations suggests that the DIN in the stream originated from the groundwater (**Fig. 9**). Maximum DIN values in the stream ranged between 300 and 400 µmol.$L^{-1}$, which was similar to the value used for the 'effective groundwater end-member' upstream ($[N]_{gw\_s}$). With the similar end-member characteristics downstream (i.e. $[N]_{gw\_d}$ = 300 ± 100 µmol.$L^{-1}$), the contribution of groundwater to the DIN flux downstream from the gauging station ranged from 56% in April (high flow) to 73% in July (low flows).

The concentration of radon in the Balaurie and Roubine canals ($C_{can}$) ranged from 2 298 to 7 664 Bq.$m^{-3}$, and their high radon and DIN concentrations were close to the values measured at the piezometers (**Fig. 9**). In addition, conductivity in the downstream part and the canals was high for all campaigns and reached the groundwater characteristics (**Fig. 6**). Since the field campaigns were conducted in dry periods, water discharging from these short canals probably only originate from groundwater and drain the lower aquifer units. Average flow in the Balaurie and Roubine canals remained between 20 L.$s^{-1}$ in dry hydrological conditions and 50 L.$s^{-1}$ in wet hydrological conditions. Consequently, canal discharge was counted as groundwater inflow, to be added to direct inflow to the main Salaison channel, meaning that groundwater contribution to total DIN flux in the downstream part was 100%.

## 3.4. Overall groundwater contribution to the inputs at Salaison outlet

At the Salaison outlet, the downstream inputs from groundwater and canals significantly increased the total DIN inputs reaching Or lagoon (i.e. $F_{station}+\Delta F_{downstream}$), which ranged from 10 tN.$y^{-1}$ (2013-2014) to 98 tN.$y^{-1}$ (2014-2015), with 59 tN.$y^{-1}$ in 2017-2018 (**Fig. 10**). The last part of the stream located in the immediate coastal environment was responsible for 44% (2014-2015) to 56% (2013-2014) of the DIN inputs to the Or lagoon, and 48% in 2017-2018.

The contribution of groundwater to annual DIN inputs at the Salaison outlet estimated with the annual groundwater-driven DIN inputs at the Salaison outlet (i.e. $F_{gw} + \Delta F_{gw}$) and DIN inputs at the Salaison outlet (i.e. $F_{station}+\Delta F_{downstream}$) ranged from 89% (2014-2015) to 94% (2013-2014). Hence, adding the results obtained from the downstream part of the Salaison to the annual DIN inputs increased the overall contribution of groundwater to this perennial stream, making it the main source of DIN in the stream.

# 4. Discussion

## 4.1. Uncertainties on the combined methods

### 4.1.1. Uncertainties on the piezometric contours

Piezometric contours were determined from measurements of the level of well water for one campaign in high flows (**Fig. 3**). The lack of information about aquifer geometry (cross-section) and hydrodynamic parameters (hydraulic transmissivity) did not allow to estimate groundwater flows using Darcy's law (Schilling and Wolter, 2007), but the method nevertheless provides a first qualitative overview of surface water / groundwater interactions around the Salaison River. Indeed, the hydraulic gradients estimated from the piezometric contours confirm the importance of the downstream part of the stream. Groundwater contributions to DIN inputs in the stream were estimated without using the groundwater catchment data, and adding a qualitative overview from a broader scale supports the conclusions of the study on the hydrogeological functioning of the area.

### 4.1.2. Uncertainties on DIN inputs upstream from the gauging station

Hydrograph separation of high frequency water flow data combined with previous stream data analysis made it possible to assess the contribution of groundwater, and the baseflow results in this study are in agreement with those of a perennial stream (Eckhardt, 2008). Our results highlight the fact that, as the main source of DIN in the stream, groundwater was diluted by a low DIN / low conductivity surface water end-member (**Fig. 5**). Nevertheless, surface driven DIN fluxes can be significant even with low DIN concentrations, especially during flood events where water flow increases significantly. Thus, considering that groundwater contribution at the gauging station was 100% would have led to an overestimation of groundwater loads.

The non-conservative relation of DIN with conductivity upstream from the gauging station suggested that using DIN concentrations in groundwater from 'theoretical' groundwater end-member would have overestimated the DIN flux upstream from the gauging station (**Fig. 5**).

455 The concentrations of DIN measured in the stream at the gauging station represent the
456 combination of DIN inputs and DIN consumption upstream, either during the transit between
457 the aquifer and the stream or during transit along the stream, for example due to uptake by
458 plants or consumption by microorganisms (Cooper, 1990). Indeed, not taking the consumption
459 processes along the stream into account would have led to a 50% overestimation (i.e. from the
460 'theoretical' end-member 600 µmol.$L^{-1}$ to the 'effective' end-members 300 µmol.$L^{-1}$). Still,
461 estimating the groundwater driven DIN flux with a constant 'effective' end-member
462 concentration deduced from groundwater samples relies on the assumption that mixing with
463 surface water is conservative. **Figure 5** shows that, in practice, this is not the case, but the
464 'effective' groundwater end-member provides a more realistic estimation of the contribution
465 of groundwater upstream. Additional data for DIN for conductivity between 800 and 1200
466 µS.$cm^{-1}$ in the stream would enable to reduce the uncertainty of the groundwater end-member
467 (i.e. conductivity associated with the 'effective groundwater end-member') (**Fig. 5**).

468 **4.1.3. Uncertainties on DIN inputs downstream from the gauging station**

469 The absolute uncertainty of groundwater inflow estimated from the radon mass balance $\Delta Q_{gw}$
470 is related to all mass balance parameters, with higher uncertainty for the April and May
471 campaigns (**Fig. 7**). The main parameters which influence uncertainty are the choice of radon
472 end-member concentrations and disscharge measurements (as initial inputs to the model).
473 Despite their high uncertainties, the model outputs (water flow at the Salaison outlet) are within
474 the same confidence intervals as manual gauging at the outlet. Importantly, the results of this
475 study suggest that all the water that discharged into the downstream part of the river was
476 groundwater driven (direct inflow + canal inputs) (**Fig. 9**). In future studies, differential water
477 flow gauging between the gauging station and the outlet would be sufficient to estimate the
478 additional groundwater flow (for periods with no significant surface flow).

Groundwater inputs downstream from the gauging station estimated in this study were extrapolated to obtain an overall DIN flux at the scale of a hydrological cycle, based on the assumption that the 7-month campaigns were representative of the whole hydrological year. Indeed, the first months of the hydrological cycle 2017-2018 were particularly dry (**Fig. 7**), with 56 mm of rainfall from September to December 2017. Furthermore, the seven campaigns were able to capture different water flows (from 55 $L.s^{-1}$ to 825 $L.s^{-1}$) which are representative of 92% of the hydrological conditions in the stream. Thus, studying water flow and changes in DIN flux in seven campaigns conducted from January to July enabled us to estimate the general interaction processes between the groundwater and the surface water for the whole hydrological cycle (from September to the following August), even though it is difficult to capture the correlation with the behaviour of the aquifer. Sampling campaigns did not capture flood events, but the results of this study show that the relative increase in high flows was not significant (**Fig. 8**). Indeed, water flow and DIN flux were already high at the gauging station and remained stable until the outlet.

#### 4.1.4. Combining methods to understand surface water / groundwater interaction in the Salaison River

In this study, complementary methods were used to improve our understanding of surface water / groundwater interactions along the Salaison River. High frequency water flow and DIN data were available for the upstream part of the Salaison, enabling the use of hydrograph baseflow separation and flow interval classification methods to estimate DIN fluxes. Downstream from the gauging station, a radon mass balance highlighted the predominance of groundwater driven DIN inputs in this part of the stream. Combining the results of the downstream radon mass balance with results of the upstream hydrograph separation results enabled estimation of groundwater-driven DIN fluxes at the Salaison outlet. Combining the methods did not reduce

503 uncertainties, but validated the robustness of the results by approaching the study from different
504 angles (Baudron et al., 2015; Martinez et al., 2015).

505 **4.2. Importance of the downstream part of the Salaison River**

506 This study demonstrated that the majority of DIN fluxes at the Salaison River outlet are
507 groundwater driven (**Fig. 10**). As a perennial stream, groundwater is a major contributor to
508 stream flow and an even more important contributor to DIN as a result of the high DIN
509 concentrations in the aquifer (Adyasari et al., 2018; Exner-Kittridge et al., 2016; Schilling et
510 al., 2018). The downstream part of the Salaison River in particular delivers 44% to 56% of the
511 DIN inputs to the Or lagoon, even though it only covers 25% of the surface watershed.
512 Moreover, inputs of groundwater downstream are less likely to be consumed before arriving at
513 the Salaison outlet compared with inputs to the upstream part of the stream, since their transit
514 time before reaching the outlet is shorter (Seitzinger, 1988).

515 In addition, the water in the two canals located downstream from the gauging station originates
516 from groundwater (**Fig. 9**). The original purpose of the two canals was to receive waste water
517 and storm water in high flow conditions (Aquascop, 2013), but they also acted as pathways
518 which enabled groundwater to reach the main channel by improving its drainage contact with
519 the aquifer (Rozemeijer and Broers, 2007). Groundwater is carried to the Salaison river through
520 these outlets, adding flow to the direct groundwater discharge which occurs all along the river.
521 The Roubine canal delivers a significant proportion of the groundwater flow (from 10 to 40
522 $L.s^{-1}$) to the last part of the Salaison River and the short transit time before reaching Or lagoon
523 limits the consumption of associated DIN fluxes.

524 Inflows of groundwater to the downstream part of the Salaison River are a major source of DIN
525 and these inputs are not monitored by the gauging station, suggesting that the position of the
526 gauging station may have a significant impact on the estimation of DIN fluxes at the Salaison

527 outlet (**Fig. 10**). Locating the Salaison gauging station 2 000 m downstream, at the limit
528 between alluvial bedrock and lagoon silt would make it possible to monitor water flow and
529 DIN concentrations more accurately while still avoiding the intrusion of lagoon water (**Fig. 3**).
530 The results of this study emphasize the need to understand surface water /groundwater
531 interactions on the continent to satisfactorily monitor nutrient fluxes to the coastal zone
532 (Delconte et al., 2014; Jin et al., 2016). Nevertheless, for the five hydrological cylces studied,
533 annual DIN inputs at the Salaison outlet were found to be correlated with annual rainfall
534 ($R^2$=0.92; $y = 0.106x - 26$, *data not shown*). Thus, available rainfall data could provide a
535 preliminary estimation of the annual load reaching the Or lagoon, as long as groundwater and
536 surface runoff constitute the main DIN sources in the stream.

537 **4.3. Groundwater is a significant source of DIN in the Or lagoon**

538 The final aim of this study was to estimate total DIN inputs from the alluvial aquifer to the Or
539 lagoon. Previous studies had concluded that no direct submarine groundwater discharge in the
540 lagoon or from other groundwater pathways from the Villafranchien aquifer to the Or lagoon
541 needed to be identified. Since geological characteristics on the northern border of the lagoon
542 at the limit with the aquifer are similar for all the northern streams, our work focused on the
543 Salaison River as a representative area for surface water / groundwater interactions. First, the
544 hydraulic gradients from the piezometric contour of the aquifer around the Salaison river
545 indicated that in high flow conditions, most of the groundwater discharges upstream from the
546 silt layer (**Fig. 3**). A change in permeability must cause groundwater outflow upstream from
547 the alluvium/silt interface (Santamaria, 1995), not only in the Salaison groundwater catchment
548 but also in the surrounding wetlands on the northern part of the lagoon (**Fig. 1a**). In these areas,
549 evaporation and plant uptake are high and man-made embankments often divide up the natural
550 areas, so the real quantity of water that arrives in the lagoon in this way may be negligible. The
551 streams thus represent the only outlets for the water table, with the Salaison River as one of the

552 main streams. Although the Salaison only accounts for 17% of the Or surface watershed, it
553 delivers 59% of total freshwater originating from the northern streams (Colin et al., 2017) and,
554 according to our results, including significant groundwater-driven inputs of DIN (> 90%) (**Fig.**
555 **10**). This study demonstrates that the Salaison River is a major conveyor of groundwater-driven
556 DIN to the Or lagoon, and is probably representative of groundwater inputs to the Or lagoon
557 from other natural streams nearby, owing to similar hydrology and hydrogeology. Moreover,
558 the important aquifer interaction with the stream could explain the important contribution of
559 the Salaison to the freshwater inputs in comparison with its small watershed.

560 To estimate groundwater driven DIN inputs from all these northern streams, two extreme
561 hydrological behaviours can be assumed. First, the Salaison can be considered as the only
562 stream fed by groundwater in the northern part of the watershed. Hence, depending on
563 hydrological conditions, this study suggests that 10 (dry hydrological cycle) to 98 $tN.y^{-1}$ (wet
564 hydrological cycle) originating from the Villafranchien aquifer reach the Or lagoon every year
565 (**Fig. 10**). It can also be assumed that all the northern streams are characterised by similar
566 surface water/groundwater interactions and DIN end-members as those of the Salaison River.
567 Since these stream supply 40% of freshwater to the Or lagoon (Colin et al., 2017), assuming
568 that 90% of this freshwater originates from groundwater, DIN inputs can be estimated. In this
569 case, 17 (dry hydrological cycle) to 163 $tN.y^{-1}$ (wet hydrological cycle) of groundwater driven
570 DIN reach the Or lagoon. Extrapolations to other northern streams involve considerable
571 uncertainties because (1) the surface water in other parts of the aquifer might constitute a
572 significant DIN source depending on land occupation, (2) the groundwater catchment of the
573 Salaison River is larger than the surface watershed, thereby reducing the aquifer system of
574 other streams including their groundwater discharge (**Fig. 3**). Despite these uncertainties, these
575 simple estimations provide an order of magnitude for total groundwater driven DIN inputs to
576 the Or lagoon, with minimum (results for the Salaison only) and maximum values.

### 4.4. Implications for managements actions in the Or lagoon

This study has shown that, even though groundwater does not discharge directly into the lagoon, groundwater-driven inputs to the inflowing stream are a significant source of DIN to the Or lagoon and are only partially taken into account in current observations made at the gauging stations. Our investigation focussed on DIN, at the origin of eutrophication - with the predominance of nitrate from the Salaison (74% to 99% of total DIN). Similar considerations apply to phosphorus or crop protection products (pesticides), for example, and, depending on concentration in the groundwater and the half-life of the molecule concerned, inputs to the coast may also be significant. This study has shown that the aquifer and its subsurface catchment have to be taken into account in territorial strategies (Adyasari et al., 2018; Stieglitz et al., 2013). This implies that the area targeted by management actions aimed at reducing inputs of the nutrient to the coastal zone has to extend from the watershed to the groundwater catchment. The residence time of water in the aquifer is another important parameter to take into account in management planning and monitoring: if the travel time is long, results of management actions will only be observed with a significant lag time (Fenton et al., 2011; van Lanen and Dijksma, 1999; Vervloet et al., 2018). Concentrations of DIN in the aquifer have remained relatively constant in the past decade, evidence that management actions in the watershed have not improved the quality of the groundwater so far. Groundwater dating should give an indication of time needed to see improvement in the nutrient concentration at the aquifer outlet (Aquilina et al., 2012).

## Conclusions

The complementary methods used in this study enabled us to investigate surface water / groundwater interactions in the upstream and downstream sections of the Salaison River. Groundwater was shown to be the main source of DIN (mainly $NO_3$) contamination of the Salaison River, thereby revealing streams to be indirect pathways for groundwater to reach the

Or lagoon. Inputs are naturally governed by hydrogeological conditions and are usually considerably underestimated when they are only measured at the gauging station. The high level of groundwater driven DIN inputs estimated in this study could inhibit restoration of the Or lagoon for many years. The results of the study improve our understanding of indirect groundwater-driven nutrient inputs from an alluvial aquifer to the coastal zone and of the land/sea continuum.

**Acknowledgements**

This research was funded by the French National Research Agency (ANR) through the ANR @RAction chair of excellence (ANR-14-ACHN-0007-01 - T Stieglitz). This research is part of a PhD projet funded by IFREMER, BRGM and CEREGE. The authors acknowledge A Nefzi, E Bousquet and S Pistre for their support with data collection and analysis. We are grateful to F Maldan (BRGM Montpellier) for all his help in the field, and also to C Saguet and L Dijoux (IFREMER Sète). DIN samples were analysed at IFREMER Sète laboratory (COFRAC - accredited) with the help of M Fortune, E Foucault and G Messiaen. We thank F Colin (SupAgro Montpellier), R De Wit (CNRS Montpellier), E Roque (IFREMER Sète), P Souchu (IFREMER Nantes) and JB Martin (University of Florida) for constructive comments on our paper. We are grateful of the two reviewers that provided useful comments to improve the manuscript.

620 **References**

621 Adyasari, D., Oehler, T., Afiati, N., Moosdorf, N., 2018. Groundwater nutrient inputs into an
622 urbanized tropical estuary system in Indonesia. Sci. Total Environ. 627, 1066–1079.
623 https://doi.org/10.1016/J.SCITOTENV.2018.01.281

624 Aminot, A., Kerouel, R., 2007. Dosage automatique des nutriments dans les eaux marines :
625 méthodes en flux continu. Editions Ifremer, 188 p.

626 Aquascop, 2013. Suivi 2012 de la qualité des eaux des bassins versants de l'étang de Thau, de
627 l'étang de l'Or, du Lez et de la Mosson. Aquascop/7197 - 307 p.

628 Aquilina, L., Vergnaud-Ayraud, V., Labasque, T., Bour, O., Molénat, J., Ruiz, L., de Montety,
629 V., De Ridder, J., Roques, C., Longuevergne, L., 2012. Nitrate dynamics in agricultural
630 catchments deduced from groundwater dating and long-term nitrate monitoring in surface-
631 and groundwaters. Sci. Total Environ. 435–436, 167–178.
632 https://doi.org/10.1016/J.SCITOTENV.2012.06.028

633 Avery, E., Bibby, R., Visser, A., Esser, B., Moran, J., 2018. Quantification of Groundwater
634 Discharge in a Subalpine Stream Using Radon-222. Water 10, 100 p.
635 https://doi.org/10.3390/w10020100

636 Banks, E.W., Simmons, C.T., Love, A.J., Shand, P., 2011. Assessing spatial and temporal
637 connectivity between surface water and groundwater in a regional catchment:
638 Implications for regional scale water quantity and quality. J. Hydrol. 404, 30–49.
639 https://doi.org/10.1016/J.JHYDROL.2011.04.017

640 Basset, A., Elliott, M., West, R.J., Wilson, J.G., 2013. Estuarine and lagoon biodiversity and
641 their natural goods and services. Estuar. Coast. Shelf Sci. 132, 1–4.
642 https://doi.org/10.1016/J.ECSS.2013.05.018

643 Baudron, P., Cockenpot, S., Lopez-Castejon, F., Radakovitch, O., Gilabert, J., Mayer, A.,
644 Garcia-Arostegui, J.L., Martinez-Vicente, D., Leduc, C., Claude, C., 2015. Combining
645 radon, short-lived radium isotopes and hydrodynamic modeling to assess submarine
646 groundwater discharge from an anthropized semiarid watershed to a Mediterranean
647 lagoon (Mar Menor, SE Spain). J. Hydrol. 525, 55–71.
648 https://doi.org/10.1016/j.jhydrol.2015.03.015

649 Blaise, M., Dorfliger, N., Le Strat, P., Ladouche, B., 2008. Etang de l'Or : relations entre les
650 eaux souterraines de l'aquifère de sub-surface et l'étang de l'Or en liaison avec
651 l'occupation du sol. BRGM/RP-55367-FR - 275 p.

652 Burnett, W.C., Aggarwal, P.K.K., Aureli, A., Bokuniewicz, H., Cable, J.E.E., Charette,
653 M.A.A., Kontar, E., Krupa, S., Kulkarni, K.M.M., Loveless, A., Moore, W.S.S.,
654 Oberdorfer, J.A.A., Oliveira, J., Ozyurt, N., Povinec, P., Privitera, A.M.G.M.G., Rajar,
655 R., Ramessur, R.T.T., Scholten, J., Stieglitz, T., Taniguchi, M., Turner, J.V. V., 2006.
656 Quantifying submarine groundwater discharge in the coastal zone via multiple methods.
657 Sci. Total Environ. 367, 498–543. https://doi.org/10.1016/j.scitotenv.2006.05.009

658 Burnett, W.C., Dulaiova, H., 2003. Estimating the dynamics of groundwater input into the
659 coastal zone via continuous radon-222 measurements. J. Environ. Radioact. 69, 21–35.
660 https://doi.org/10.1016/S0265-931X(03)00084-5

661 Burnett, W.C., Taniguchi, M., Oberdorfer, J., 2001. Measurement and significance of the direct
662 discharge of groundwater into the coastal zone. J. Sea Res. 46, 109–116.
663 https://doi.org/10.1016/S1385-1101(01)00075-2

664 Chapman, T., 1999. A comparison of algorithms for stream flow recession and baseflow
665 separation. Hydrol. Process. 13, 701–714. https://doi.org/10.1002/(SICI)1099-
666 1085(19990415)13:5<701::AID-HYP774>3.0.CO;2-2

667 Charette, M.A., Buesseler, K.O., Andrews, J.E., 2001. Utility of radium isotopes for evaluating
668 the input and transport of groundwater-derived nitrogen to a Cape Cod estuary. Limnol.
669 Oceanogr. 46, 465–470. https://doi.org/10.4319/lo.2001.46.2.0465

670 Cloern, J.E., 2001. Our evolving conceptual model of the coastal eutrophication problem. Mar.
671 Ecol. Prog. Ser. https://doi.org/10.3354/meps210223

672 Colin, F., Crabit, A., Augas, J., Garnier, F., Favre, L., Lilti, V., Verlingue, U., 2017. Apports
673 d'eau aux lagunes côtières méditerranéennes - Propositions méthodologiques pour la
674 quantification des écoulements basées sur des mesures légères et des modèles
675 synthétiques. Rapport de fin de projet Agence de l'Eau RMC. Montpellier SupAgro - 50
676 p.

677 Cook, P.G., Favreau, G., Dighton, J.C., Tickell, S., 2003. Determining natural groundwater
678 influx to a tropical river using radon, chlorofluorocarbons and ionic environmental tracers.
679 J. Hydrol. 277, 74–88. https://doi.org/10.1016/S0022-1694(03)00087-8

680 Cook, P.G., Lamontagne, S., Berhane, D., Clark, J.F., 2006. Quantifying groundwater
681 discharge to Cockburn River, southeastern Australia, using dissolved gas tracers 222 Rn
682 and SF 6. Water Resour. Res. 42. https://doi.org/10.1029/2006WR004921

683 Cook, P.G., Wood, C., White, T., Simmons, C.T., Fass, T., Brunner, P., 2008. Groundwater
684 inflow to a shallow, poorly-mixed wetland estimated from a mass balance of radon. J.
685 Hydrol. 354, 213–226. https://doi.org/10.1016/j.jhydrol.2008.03.016

686 Cooper, A.B., 1990. Nitrate depletion in the riparian zone and stream channel of a small
687 headwater catchment. Hydrobiologia 202, 13–26. https://doi.org/10.1007/BF00027089

688 de Jonge, V.N., Elliott, M., Orive, E., 2002. Causes, historical development, effects and future
689 challenges of a common environmental problem: eutrophication. Hydrobiologia 475/476,

690 1–19. https://doi.org/10.1023/A:1020366418295

691 Delconte, C.A., Sacchi, E., Racchetti, E., Bartoli, M., Mas-Pla, J., Re, V., 2014. Nitrogen inputs
692 to a river course in a heavily impacted watershed: A combined hydrochemical and isotopic
693 evaluation (Oglio River Basin, N Italy). Sci. Total Environ. 466–467, 924–938.
694 https://doi.org/10.1016/J.SCITOTENV.2013.07.092

695 Derolez, V., Fiandrino, A., Munaron, D., 2014. Bilan sur les principales pressions pesant sur
696 les lagunes méditerranéennes et leurs liens avec l'état DCE. Rapport Ifremer/RST-
697 LER/LR 14-20 - 46 p.

698 Derolez, V., Gimard, A., Munaron, D., Ouisse, V., Messiaen, G., Fortune, M., Poirrier, S.,
699 Mortreux, S., Guillou, J.-L., Brun, M., Provost, C., Hatey, E., Bec, B., Malet, N.,
700 Fiandrino, A., 2017. OBSLAG 2016 - volet eutrophisation. Etat DCE des lagunes
701 méditerranéennes (eau et phytoplancton, période 2011-2016). Développement
702 d'indicateurs de tendance et de variabilité. Ifremer/RST/LER/LR/17.10 - 75 p.

703 Eckhardt, K., 2008. A comparison of baseflow indices, which were calculated with seven
704 different baseflow separation methods. J. Hydrol. 352, 168–173.
705 https://doi.org/10.1016/j.jhydrol.2008.01.005

706 Eckhardt, K., 2005. How to construct recursive digital filters for baseflow separation. Hydrol.
707 Process. 19, 507–515. https://doi.org/10.1002/hyp.5675

708 Exner-Kittridge, M., Strauss, P., Blöschl, G., Eder, A., Saracevic, E., Zessner, M., 2016. The
709 seasonal dynamics of the stream sources and input flow paths of water and nitrogen of an
710 Austrian headwater agricultural catchment. Sci. Total Environ. 542, 935–945.
711 https://doi.org/10.1016/J.SCITOTENV.2015.10.151

712 Fenton, O., Schulte, R.P.O., Jordan, P., Lalor, S.T.J., Richards, K.G., 2011. Time lag: a

713 methodology for the estimation of vertical and horizontal travel and flushing timescales
714 to nitrate threshold concentrations in Irish aquifers. Environ. Sci. Policy 14, 419–431.
715 https://doi.org/10.1016/J.ENVSCI.2011.03.006

716 Jin, L., Whitehead, P.G., Heppell, C.M., Lansdown, K., Purdie, D.A., Trimmer, M., 2016.
717 Modelling flow and inorganic nitrogen dynamics on the Hampshire Avon: Linking
718 upstream processes to downstream water quality. Sci. Total Environ. 572, 1496–1506.
719 https://doi.org/10.1016/J.SCITOTENV.2016.02.156

720 Johannes, R., 1980. The Ecological Significance of the Submarine Discharge of Groundwater.
721 Mar. Ecol. Prog. Ser. 3, 365–373. https://doi.org/10.3354/meps003365

722 Khadka, M.B., Martin, J.B., Kurz, M.J., 2017. Synoptic estimates of diffuse groundwater
723 seepage to a spring-fed karst river at high spatial resolution using an automated radon
724 measurement technique. J. Hydrol. 544, 86–96.
725 https://doi.org/10.1016/J.JHYDROL.2016.11.013

726 Kjerfve, B., Magill, K.., 1989. Geographic and hydrodynamic characteristics of shallow coastal
727 lagoons. Mar. Geol. 88, 187–199. https://doi.org/10.1016/0025-3227(89)90097-2

728 Lanini, S., Caballero, Y., Seguin, J.-J., Maréchal, J.-C., 2016. ESPERE-A Multiple-Method
729 Microsoft Excel Application for Estimating Aquifer Recharge. Groundwater 54, 155–156.
730 https://doi.org/10.1111/gwat.12390

731 Martinez, J.L., Raiber, M., Cox, M.E., 2015. Assessment of groundwater–surface water
732 interaction using long-term hydrochemical data and isotope hydrology: Headwaters of the
733 Condamine River, Southeast Queensland, Australia. Sci. Total Environ. 536, 499–516.
734 https://doi.org/10.1016/J.SCITOTENV.2015.07.031

735 Meinesz, C., Derolez, V., Bouchoucha, M., 2013. Base de données « pressions sur les lagunes

méditerranéennes ». Analyse des liens état – pression, Rapport Ifremer RST.ODE/LER-PAC/13-11 - 71 p.

Menció, A., Galán, M., Boix, D., Mas-Pla, J., 2014. Analysis of stream–aquifer relationships: A comparison between mass balance and Darcy's law approaches. J. Hydrol. 517, 157–172. https://doi.org/10.1016/J.JHYDROL.2014.05.039

Mooney, H., Larigauderie, A., Cesario, M., Elmquist, T., Hoegh-Guldberg, O., Lavorel, S., Mace, G.M., Palmer, M., Scholes, R., Yahara, T., 2009. Biodiversity, climate change, and ecosystem services. Curr. Opin. Environ. Sustain. 1, 46–54. https://doi.org/10.1016/J.COSUST.2009.07.006

Moore, W.S., 2010. The Effect of Submarine Groundwater Discharge on the Ocean. Ann. Rev. Mar. Sci. 2, 59–88. https://doi.org/10.1146/annurev-marine-120308-081019

Mullinger, N.J., Binley, A.M., Pates, J.M., Crook, N.P., 2007. Radon in Chalk streams: Spatial and temporal variation of groundwater sources in the Pang and Lambourn catchments, UK. J. Hydrol. 339, 172–182. https://doi.org/10.1016/J.JHYDROL.2007.03.010

Newton, A., Brito, A.C., Icely, J.D., Derolez, V., Clara, I., Angus, S., Schernewski, G., Inácio, M., Lillebø, A.I., Sousa, A.I., Béjaoui, B., Solidoro, C., Tosic, M., Cañedo-Argüelles, M., Yamamuro, M., Reizopoulou, S., Tseng, H.-C., Canu, D., Roselli, L., Maanan, M., Cristina, S., Ruiz-Fernández, A.C., Lima, R.F. de, Kjerfve, B., Rubio-Cisneros, N., Pérez-Ruzafa, A., Marcos, C., Pastres, R., Pranovi, F., Snoussi, M., Turpie, J., Tuchkovenko, Y., Dyack, B., Brookes, J., Povilanskas, R., Khokhlov, V., 2018. Assessing, quantifying and valuing the ecosystem services of coastal lagoons. J. Nat. Conserv. 44, 50–65. https://doi.org/10.1016/J.JNC.2018.02.009

Newton, A., Icely, J., Cristina, S., Brito, A., Cardoso, A.C., Colijn, F., Riva, S.D., Gertz, F., Hansen, J.W., Holmer, M., Ivanova, K., Leppäkoski, E., Canu, D.M., Mocenni, C.,

760 Mudge, S., Murray, N., Pejrup, M., Razinkovas, A., Reizopoulou, S., Pérez-Ruzafa, A.,
761 Schernewski, G., Schubert, H., Carr, L., Solidoro, C., PierluigiViaroli, Zaldívar, J.-M.,
762 2014. An overview of ecological status, vulnerability and future perspectives of European
763 large shallow, semi-enclosed coastal systems, lagoons and transitional waters. Estuar.
764 Coast. Shelf Sci. 140, 95–122. https://doi.org/10.1016/J.ECSS.2013.05.023

765 Peterson, R.N., Santos, I.R., Burnett, W.C., 2010. Evaluating groundwater discharge to tidal
766 rivers based on a Rn-222 time-series approach. Estuar. Coast. Shelf Sci. 86, 165–178.
767 https://doi.org/10.1016/J.ECSS.2009.10.022

768 Quintana, X.D., Moreno-Amich, R., Comín, F.A., 1998. Nutrient and plankton dynamics in a
769 Mediterranean salt marsh dominated by incidents of flooding. Part 1: Differential
770 confinement of nutrients. J. Plankton Res. 20, 2089–2107.
771 https://doi.org/10.1093/plankt/20.11.2089

772 Rimmelin, P., Dumon, J.-C., Maneux, E., Gonçalves, A., 1998. Study of Annual and Seasonal
773 Dissolved Inorganic Nitrogen Inputs into the Arcachon Lagoon, Atlantic Coast (France).
774 Estuar. Coast. Shelf Sci. 47, 649–659. https://doi.org/10.1006/ECSS.1998.0384

775 Rodellas, V., Garcia-Orellana, J., Masqué, P., Feldman, M., Weinstein, Y., 2015. Submarine
776 groundwater discharge as a major source of nutrients to the Mediterranean Sea. Proc. Natl.
777 Acad. Sci. U. S. A. 112, 3926–30. https://doi.org/10.1073/pnas.1419049112

778 Rodellas, V., Stieglitz, T.C., Andrisoa, A., Cook, P.G., Raimbault, P., Tamborski, J.J., van
779 Beek, P., Radakovitch, O., 2018. Groundwater-driven nutrient inputs to coastal lagoons:
780 The relevance of lagoon water recirculation as a conveyor of dissolved nutrients. Sci.
781 Total Environ. 642, 764–780. https://doi.org/10.1016/J.SCITOTENV.2018.06.095

782 Rozemeijer, J.C., Broers, H.P., 2007. The groundwater contribution to surface water
783 contamination in a region with intensive agricultural land use (Noord-Brabant, The

784 Netherlands). Environ. Pollut. 148, 695–706.
785 https://doi.org/10.1016/J.ENVPOL.2007.01.028

786 Santamaria, L., 1995. Etude preliminaire des transferts d'eau et de solutés à l'étang de l'Or, au
787 travers des formations villafranchiennes dans la plaine de Mauguio-Lunel, interface
788 nappe-étang. Université Montpellier II/ Mémoire de fin d'études - 46 p.

789 Santos, I.R., Peterson, R.N., Eyre, B.D., Burnett, W.C., 2010. Significant lateral inputs of fresh
790 groundwater into a stratified tropical estuary: Evidence from radon and radium isotopes.
791 Mar. Chem. 121, 37–48. https://doi.org/10.1016/J.MARCHEM.2010.03.003

792 Schilling, K.E., Streeter, M.T., Bettis, E.A., Wilson, C.G., Papanicolaou, A.N., 2018.
793 Groundwater monitoring at the watershed scale: An evaluation of recharge and nonpoint
794 source pollutant loading in the Clear Creek Watershed, Iowa. Hydrol. Process. 32, 562–
795 575. https://doi.org/10.1002/hyp.11440

796 Schilling, K.E., Wolter, C.F., 2007. A GIS-based groundwater travel time model to evaluate
797 stream nitrate concentration reductions from land use change. Environ. Geol. 53, 433–
798 443. https://doi.org/10.1007/s00254-007-0659-0

799 Schilling, K.E., Wolter, C.F., 2001. Contribution of Base Flow to Nonpoint Source Pollution
800 Loads in an Agricultural Watershed. Ground Water 39, 49–58.
801 https://doi.org/10.1111/j.1745-6584.2001.tb00350.x

802 Seitzinger, S.P., 1988. Denitrification in freshwater and coastal marine ecosystems: Ecological
803 and geochemical significance. Limnol. Oceanogr. 33, 702–724.
804 https://doi.org/10.4319/lo.1988.33.4part2.0702

805 Slomp, C.P., Van Cappellen, P., 2004. Nutrient inputs to the coastal ocean through submarine
806 groundwater discharge: controls and potential impact. J. Hydrol. 295, 64–86.

807 https://doi.org/10.1016/j.jhydrol.2004.02.018

808 Souchu, P., Bec, B., Smith, V.H., Laugier, T., Fiandrino, A., Benau, L., Orsoni, V., Collos, Y.,
809 Vaquer, A., 2010. Patterns in nutrient limitation and chlorophyll a along an anthropogenic
810 eutrophication gradient in French Mediterranean coastal lagoons. Can. J. Fish. Aquat. Sci.
811 67, 743–753. https://doi.org/10.1139/F10-018

812 Stieglitz, T.C., van Beek, P., Souhaut, M., Cook, P.G., 2013. Karstic groundwater discharge
813 and seawater recirculation through sediments in shallow coastal Mediterranean lagoons,
814 determined from water, salt and radon budgets. Mar. Chem. 156, 73–84.
815 https://doi.org/10.1016/j.marchem.2013.05.005

816 Symbo, 2017. Tableau de bord de suivi environnemental du contrat de bassin de l'Or. OUTIL
817 TECHNIQUE TBSE – Or 2017 - 33 p.

818 Symbo, 2014. Le Salaison, état des lieux et programme pluriannuel de gestion et de
819 restauration. 30 p.

820 Taylor, D., Nixon, S., Granger, S., Buckley, B., 1995. Nutrient limitation and the
821 eutrophication of coastal lagoons. Mar. Ecol. Prog. Ser. 127, 235–244.
822 https://doi.org/10.3354/meps127235

823 van Lanen, H.A.J., Dijksma, R., 1999. Water flow and nitrate transport to a groundwater-fed
824 stream in the Belgian-Dutch chalk region. Hydrol. Process. 13, 295–307.
825 https://doi.org/10.1002/(SICI)1099-1085(19990228)13:3<295::AID-HYP739>3.0.CO;2-
826 O

827 Vervloet, L.S.C., Binning, P.J., Børgesen, C.D., Højberg, A.L., 2018. Delay in catchment
828 nitrogen load to streams following restrictions on fertilizer application. Sci. Total Environ.
829 627, 1154–1166. https://doi.org/10.1016/J.SCITOTENV.2018.01.255

830

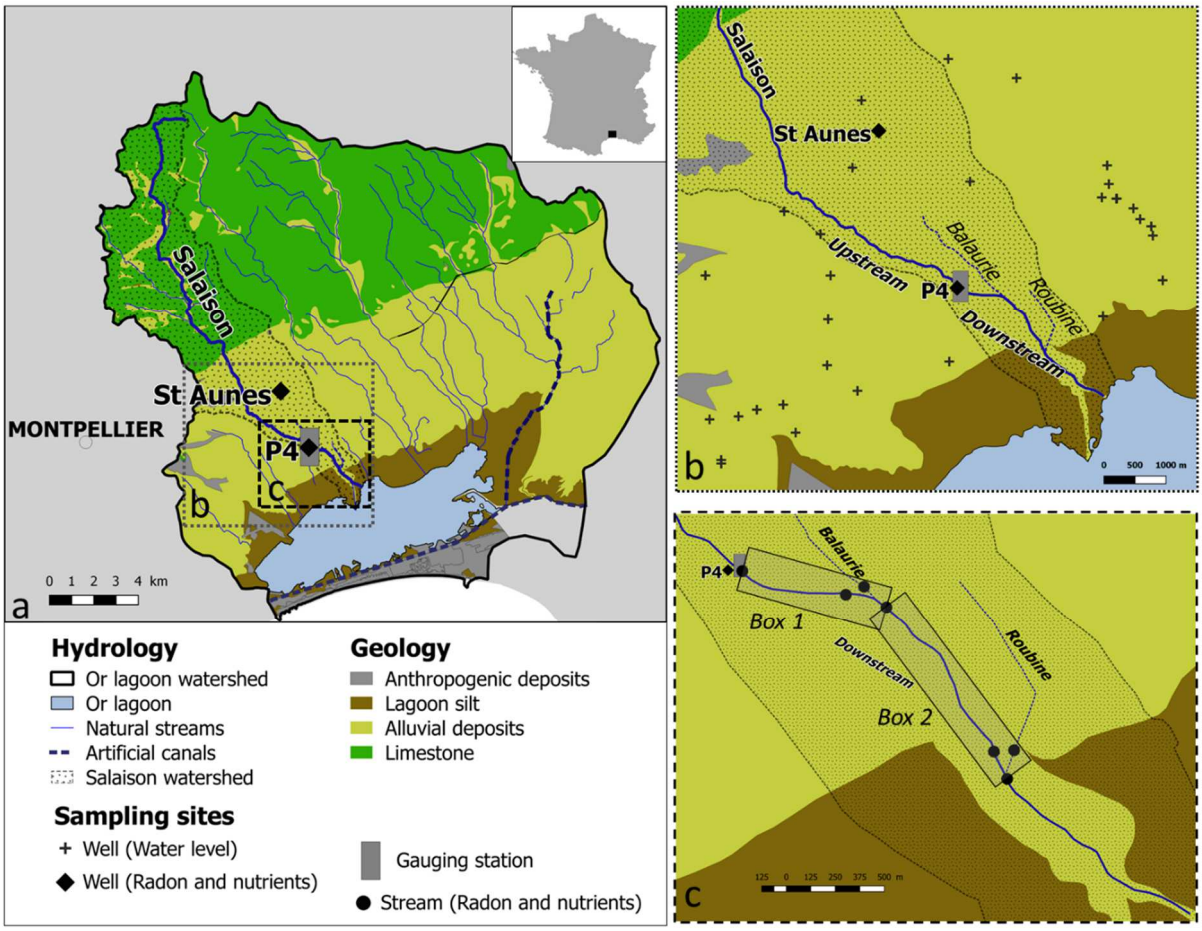


**Figure 1**: a) Hydrogeological settings and localisation of piezometers for the study site; b) Sampling stations for the piezometric map (water levelled wells) and localisation of the gauging station in Salaison river; c) Sampling sites for the radon sampling downstream of the gauging station and the two associated box models for the radon mass balance.

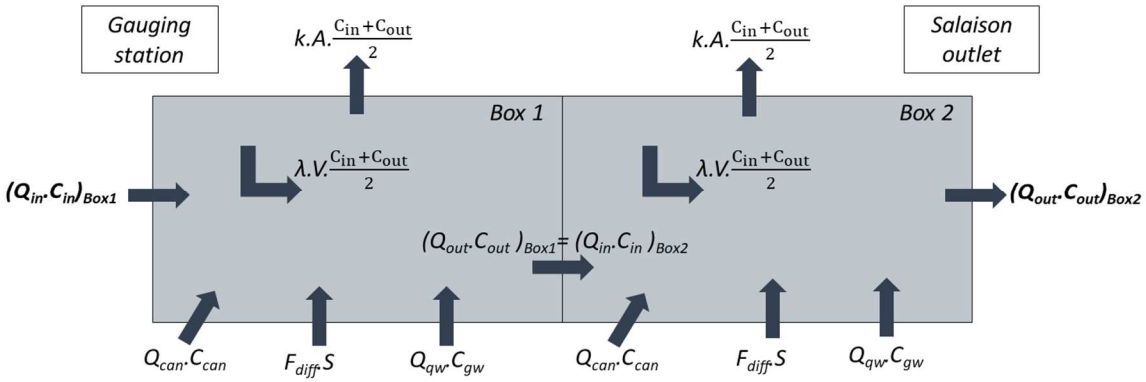


**Figure 2**: Conceptual scheme of the connected boxes for the radon mass balance in the downstream part of Salaison River: sinks and sources of radon flux ($Bq.s^{-1}$)

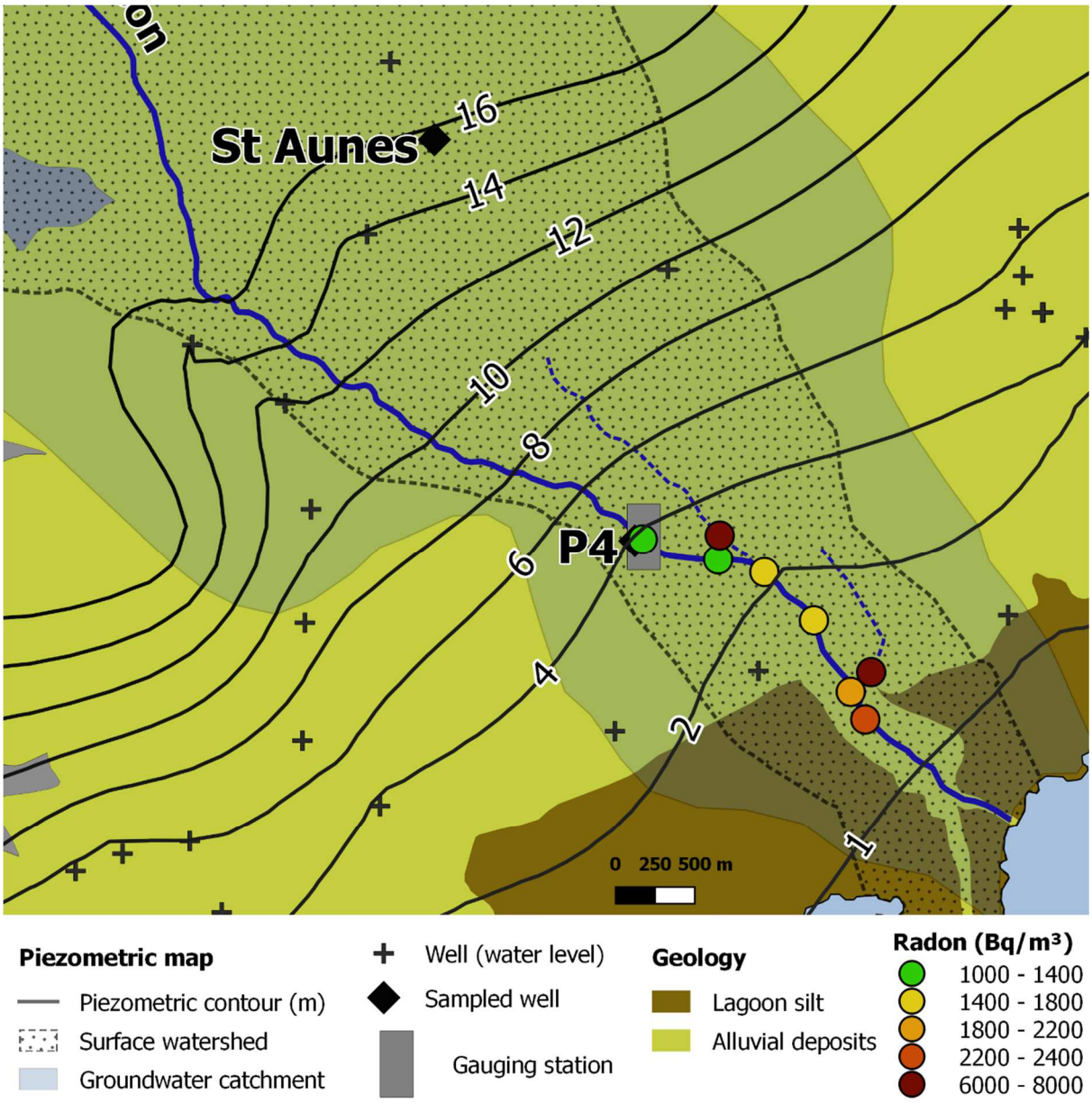


**Figure 3**: Piezometric maps describing Salaison's groundwater catchment. Salaison watershed is displayed for comparison with the groundwater catchment. On the downstream part of Salaison River, an example of radon concentrations measured on 2/15/2018 is presented, showing significant radon increase due to significant groundwater input downstream.

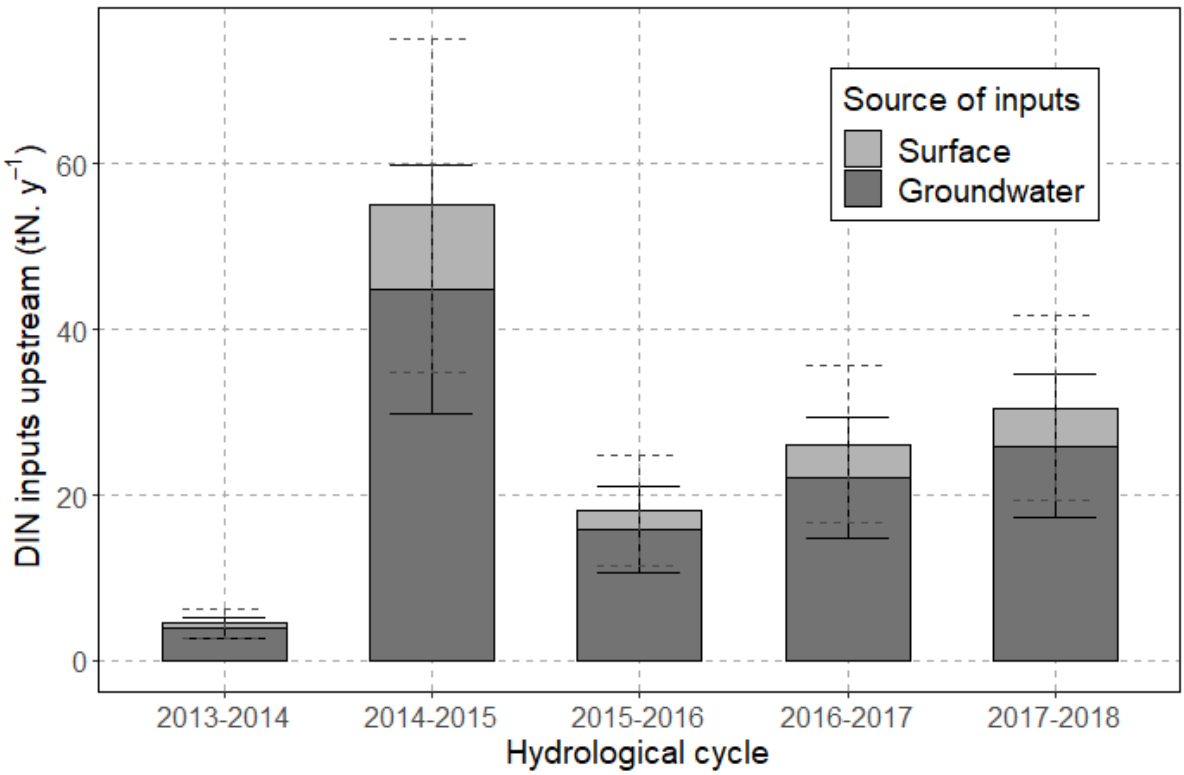


**Figure 4**: DIN inputs at the gauging station assessed from the flow interval method with data from Salaison gauging station monitoring (combining all sources), and groundwater contribution to the total DIN inputs estimated from baseflow separation and end-member mixing analysis (dark grey).

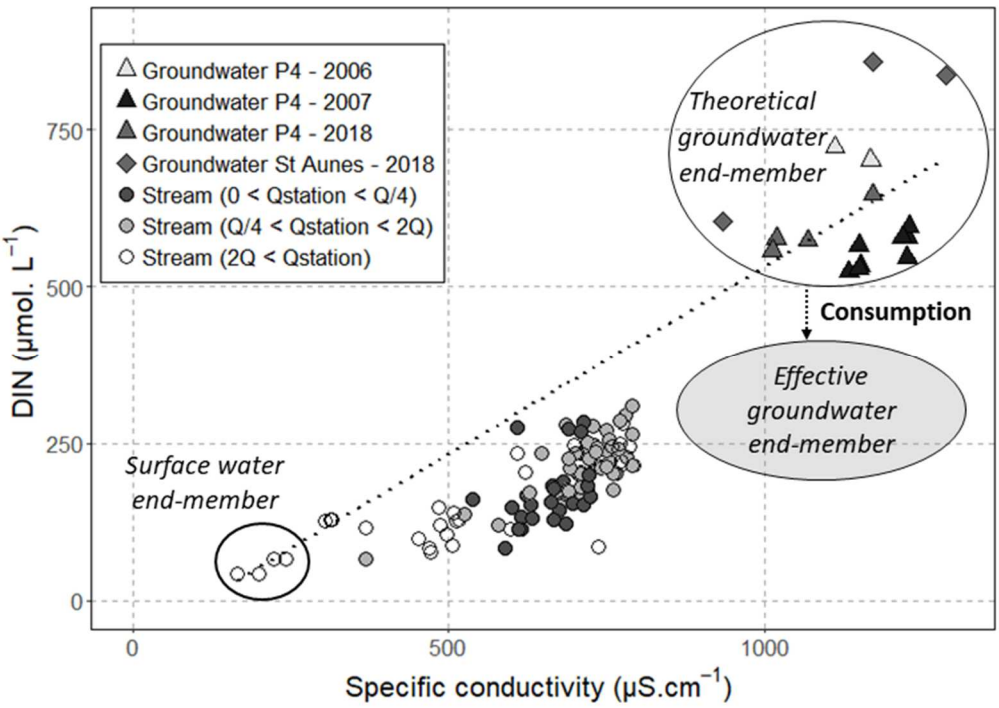


**Figure 5**: DIN evolution (µmol.$L^{-1}$) according to specific conductivity (µS.$cm^{-1}$) measured at Salaison gauging station from 2013 to 2018 (circles) for different water flow classes (in L.$s^{-1}$) (detailed in Table 2), and in the piezometer P4 in 2006 (square), 2007 (diamond) and 2018 (triangle). Dotted black line represents the hypothetical conservative mixing line between high conductivity/high DIN end-member and low conductivity/low DIN end-member.

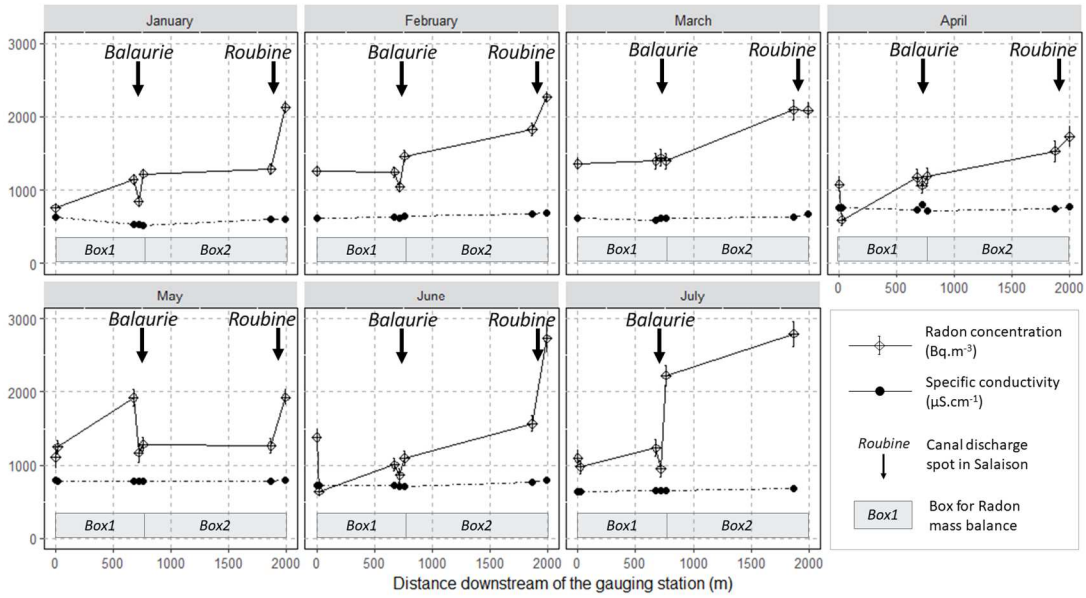


**Figure 6**: Radon concentration ($Bq.m^{-3}$) and specific conductivity ($\mu S.cm^{-1}$) in the downstream part of the river measured during each campaign in 2018. Grey boxes show the extent of radon mass balance implemented.

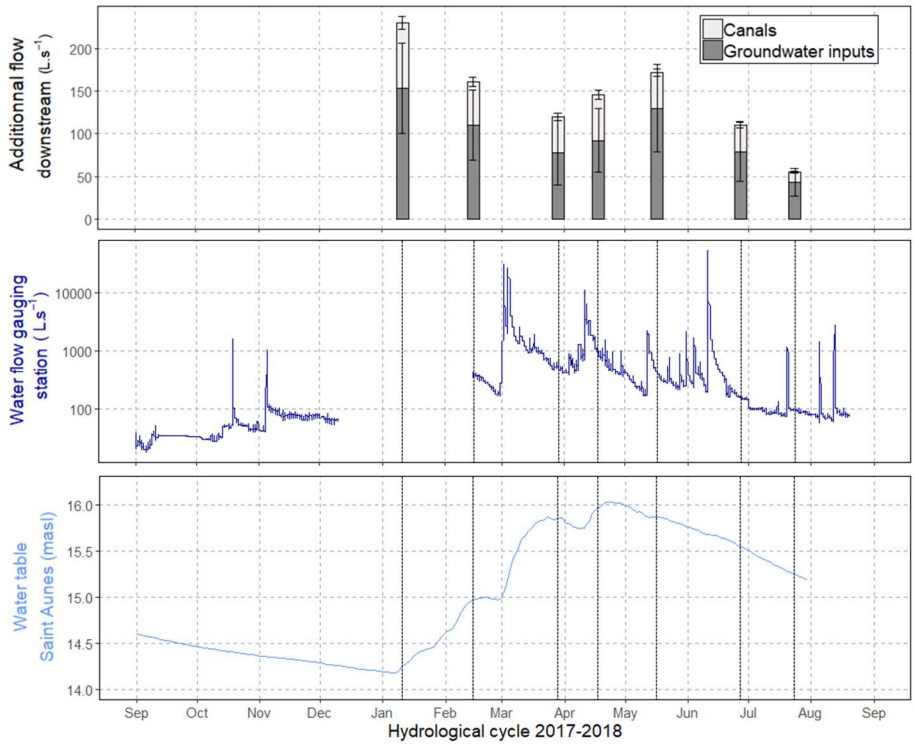


**Figure 7:** Groundwater discharge in the downstream part of Salaison River ($L.s^{-1}$) assessed with the radon mass balance in 2018 (top); water flow at Salaison gauging station ($L.s^{-1}$) (middle); water table fluctuation (m) at Saint Aunes piezometer (bottom). Vertical lines show campaign periods.

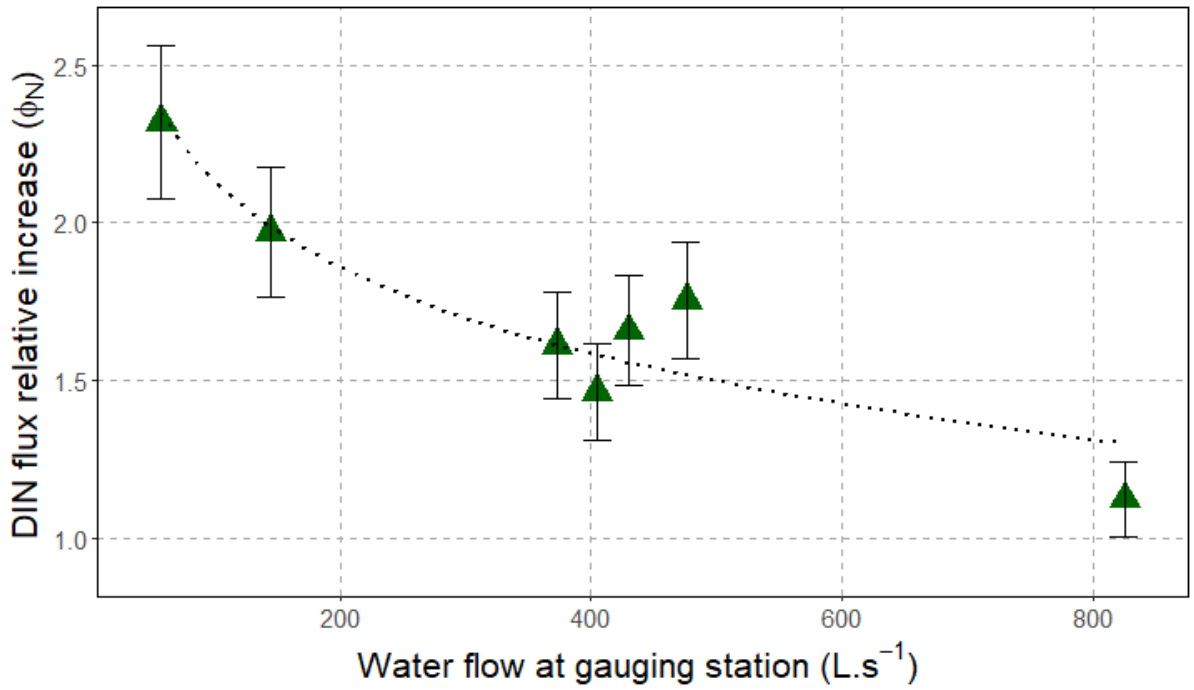


**Figure 8:** Increase factor of DIN flux downstream from the gauging station according to hydrological conditions at the gauging station (L.s$^{-1}$).

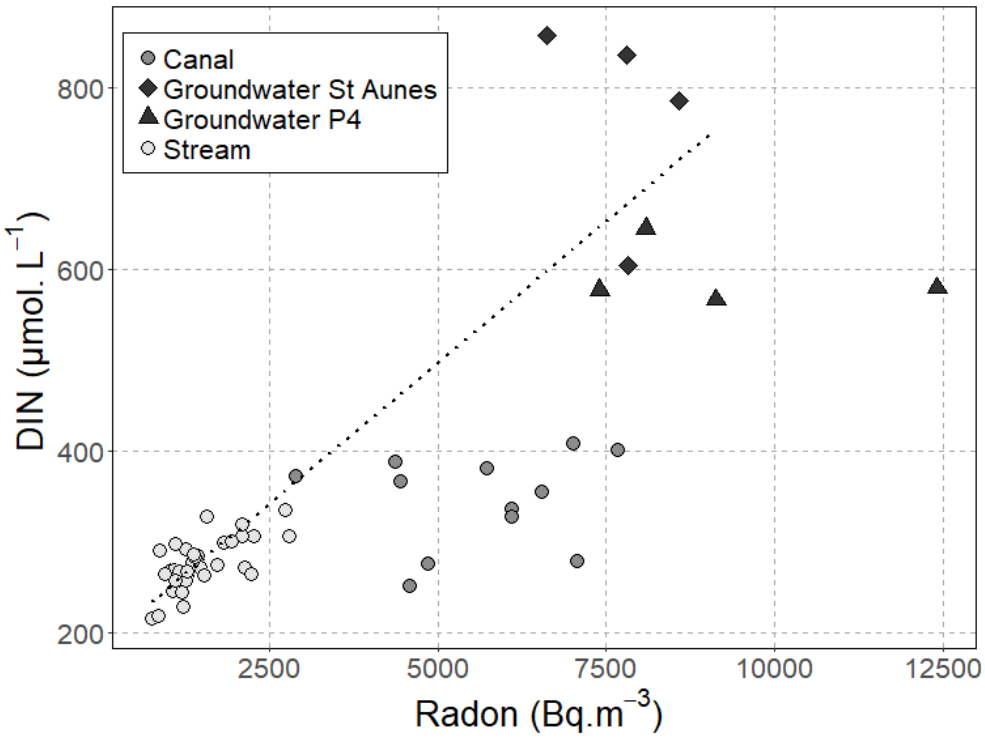


**Figure 9:** DIN concentrations (µmol.L$^{-1}$) according to radon concentration (Bq.m$^3$) in the downstream part of Salaison river measured during each campaign in 2018 in the stream (filled circles), in the two canals (hollow circles) and in piezometer P4 (diamonds).

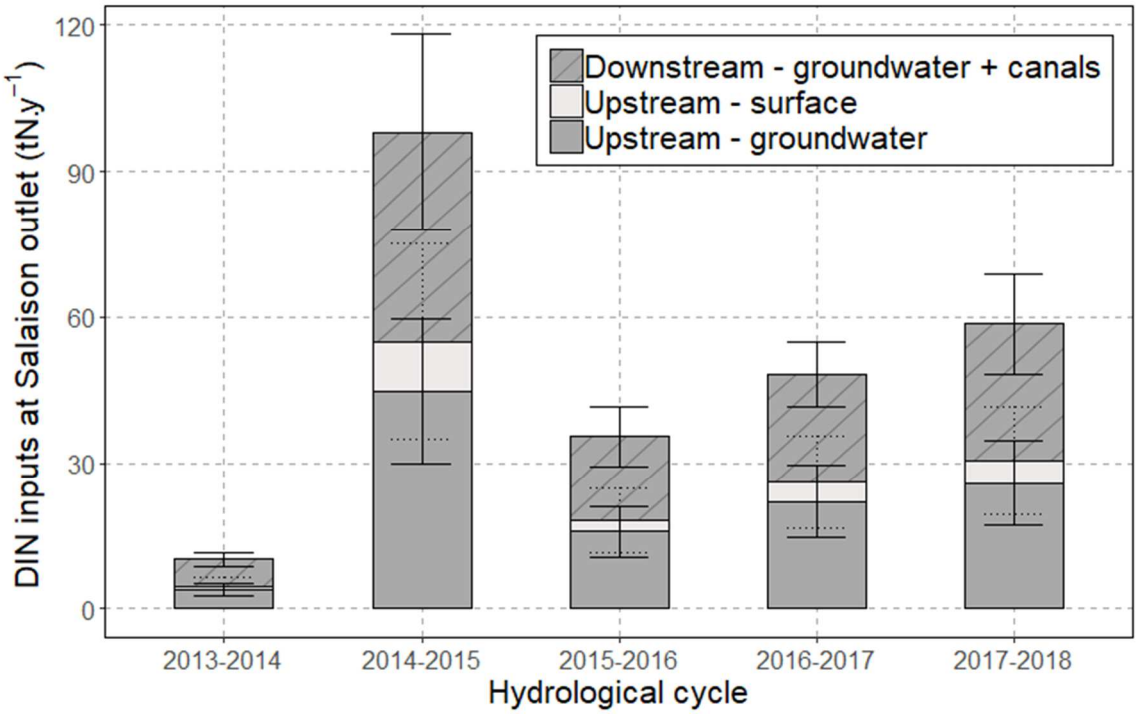


**Figure 10:** Estimation of DIN inputs to Or lagoon at Salaison outlet: upstream inputs estimated at the gauging station integrating groundwater-driven DIN inputs (dark grey) and surface-driven DIN inputs (light grey); additional groundwater-driven DIN inputs discharging downstream of the gauging station in the river and through the canals (dark grey with oblique lines).

| | | Upstream | Downstream |
|---|---|---|---|
| **Total DIN flux** | Waterflow | Data available at the gauging station from 2013 to 2018 - $\mathbf{Q_{station}}$ | Radon mass balance – $\mathbf{\Delta Q_{downstream}}$ (Table 3, fig. 6 and 7) |
| | DIN concentration | Data available at the gauging station from 2013 to 2018 – $\mathbf{[N]_{station}}$ (Fig 5) | Field sampling (Fig 9) |
| **Groundwater driven DIN flux** | Groundwater flow | Baseflow separation - $\mathbf{Q_{gw}}$ | Radon mass balance - $\mathbf{\Delta Q_{gw}}$ (Table 3, fig. 6 and 7) |
| | DIN groundwater end-member | Conductivity/DIN correlation– $\mathbf{[N]_{gw\_s}}$ (Fig 5) | Radon/DIN correlation – $\mathbf{[N]_{gw\_d}}$ (Fig 9) |

**Table 1**: Review of the different methods implemented to study DIN inputs in Salaison River. For each variable, the table presents the origin of the data, the variable name in the study (in bold) and the associated figures showing the data.

| **Water flow class** | **Average DIN ($[N]_{station}$) ($\mu mol.L^{-1}$)** | **Standard deviation ($\mu mol.L^{-1}$)** |
|---|---|---|
| $0 < Q_{station} < Q/4$ | $\mu = 170$ | $\sigma = 62$ |
| $Q/4 < Q_{station} < 2Q$ | $\mu = 220$ | $\sigma = 64$ |
| $2Q < Q_{station}$ | $\mu = 110$ | $\sigma = 59$ |

**Table 2**: Flow classes and associated average DIN concentrations (source: DREAL) to estimate total nitrogen flux on the upstream part of Salaison river. Classes for each high-frequency water flow ($Q_{station}$) were determined according to average water flow Q (386 $L.s^{-1}$) at the gauging station.

| | | | January | | February | | March | | April | | May | | June | | July | |
|---|---|---|---|---|---|---|---|---|---|---|---|---|---|---|---|---|
| | | | Box 1 | Box 2 | Box 1 | Box 2 | Box 1 | Box 2 | Box 1 | Box 2 | Box 1 | Box 2 | Box 1 | Box 2 | Box 1 | Box 2 |
| **Radon sources** | Inflow upstream | Water flow **Qin** ($L.s^{-1}$) | 476 | 529 | 430 | 480 | 405 | 425 | 825 | 854 | 371 | 408 | 145 | 155 | 58 | 87 |
| | | Radon concentration **Cin** ($Bq.m^{-3}$) | 756 | 1217 | 1255 | 1463 | 1354 | 1393 | 1075 | 1190 | 1107 | 1285 | 1378 | 1096 | 1095 | 2224 |
| | Inflow from canal | Water flow **Qcan** ($L.s^{-1}$) | 19 | 58 | 12 | 39 | 10 | 32 | 12 | 42 | 9 | 31 | 12 | 19 | 12 | - |
| | | Radon concentration **Ccan** ($Bq.m^{-3}$) | 4842 | 4358 | 6545 | 7665 | 6095 | 7016 | 4842 | 4358 | 6094 | 2883 | 4569 | 4441 | 2299 | - |
| | Diffusion from sediments | Diffusion flux **Fdiff** ($Bq.m^{2}.s^{-1}$) | 6,9E-03 | 6,9E-03 | 6,9E-03 | 6,9E-03 | 6,9E-03 | 6,9E-03 | 6,9E-03 | 6,9E-03 | 6,9E-03 | 6,9E-03 | 6,9E-03 | 6,9E-03 | 6,9E-03 | 6,9E-03 |
| | | Sediment surface **S** ($m^2$) | 5410 | 11888 | 6705 | 12093 | 5182 | 12093 | 6553 | 12217 | 6401 | 12093 | 5029 | 11229 | 5029 | 6205 |
| | Inflow from groundwater | Water flow **Qgw** ($L.s^{-1}$) | model output | | | | | | | | | | | | | |
| | | Radon concentration **Cgw** ($Bq.m^{-3}$) | 8087 | 8087 | 8087 | 8087 | 9132 | 9132 | 9132 | 9132 | 9158 | 9158 | 10212 | 10212 | 12411 | 12411 |
| **Radon sinks** | Decay | Decay constant **ƛ** ($s^{-1}$) | 2,1E-06 | 2,1E-06 | 2,1E-06 | 2,1E-06 | 2,1E-06 | 2,1E-06 | 2,1E-06 | 2,1E-06 | 2,1E-06 | 2,1E-06 | 2,1E-06 | 2,1E-06 | 2,1E-06 | 2,1E-06 |
| | | Box water volume **V** ($m^3$) | 2324 | 8699 | 3227 | 8884 | 2389 | 8885 | 3383 | 9378 | 5819 | 8885 | 1955 | 5430 | 1955 | 2742 |
| | | Average Radon concentration ($Bq.m^{-3}$) | 987 | 1671 | 1359 | 1864 | 1374 | 1741 | 1133 | 1460 | 1196 | 1606 | 1237 | 1913 | 1660 | 2509 |
| | Atmospheric evasion | Evasion coefficient **k** ($m.s^{-1}$) | 2,5E-05 | 2,5E-05 | 1,6E-05 | 1,6E-05 | 2,3E-05 | 2,3E-05 | 1,9E-05 | 1,9E-05 | 2,5E-05 | 2,5E-05 | 1,9E-05 | 1,9E-05 | 1,9E-05 | 1,9E-05 |
| | | Water surface **A** ($m^2$) | 4648 | 9666 | 5867 | 9872 | 4343 | 9872 | 5638 | 9872 | 5639 | 9872 | 4343 | 9872 | 4343 | 4986 |
| | | Average Radon concentration ($Bq.m^{-3}$) | 987 | 1671 | 1359 | 1864 | 1374 | 1741 | 1133 | 1460 | 1196 | 1606 | 1237 | 1913 | 1660 | 2509 |
| | Outflow downstream | Water flow Qout ($L.s^{-1}$) | model output | | | | | | | | | | | | | |
| | | Radon concentration **Cout** ($Bq.m^{-3}$) | 1217 | 2124 | 1463 | 2264 | 1393 | 2088 | 1190 | 1729 | 1285 | 1927 | 1096 | 2730 | 2224 | 2793 |
| **Radon mass balance outputs** | | **Water flowing out Qout ($L.s^{-1}$)** | **529** | **654** | **480** | **591** | **425** | **526** | **854** | **971** | **408** | **545** | **155** | **255** | **87** | **113** |
| | | **Groundwater discharge Qgw ($L.s^{-1}$)** | **34** | **119** | **38** | **73** | **10** | **69** | **17** | **76** | **26** | **106** | **-2** | **80** | **17** | **26** |

**Table 3**: Sources and sinks of the radon mass balance used in each campaign of this study. Water inflow in box 1 presented here corresponds to the manual measurements at the gauging station; diffusion from sediment was estimated in one sampling and the same value were applied in each campaign; atmospheric evasion was evaluated at each campaign; groundwater radon concentrations corresponds to the nearest radon measurements made in P4 piezometer.

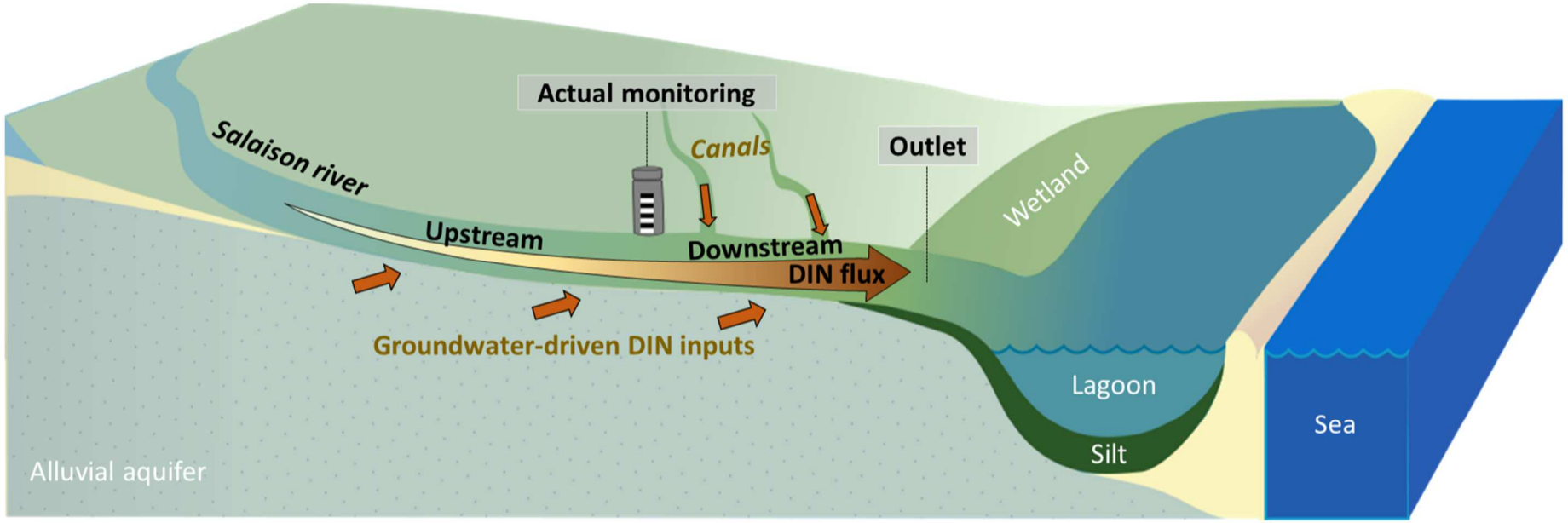
Actual monitoring
Salaison river
Canals
Outlet
Wetland
Upstream
Downstream
DIN flux
Groundwater-driven DIN inputs
Lagoon
Sea
Silt
Alluvial aquifer